Engineering Structures 249 (2021) 113362

Contents lists available at ScienceDirect

Engineering Structures

journal homepage: www.elsevier.com/locate/engstruct

Influence of bond-slip on the flexural performance and ductility of steel fibres-reinforced RC beams with lap-spliced bars: Experimental and finite element analysis

Arash Karimipour [a], Jorge de Brito [b,*], Osman Gencel [c]

[a] Department of Civil Engineering at University of Texas at El Paso and a Member of Centre for Transportation Infrastructure Systems (CTIS), TX, USA
[b] Department of Civil Engineering, Architecture and Georresources, Instituto Superior Técnico, Universidade de Lisboa, 1649-004, Portugal
[c] Civil Engineering Department, Faculty of Engineering, Bartin University, 74100 Bartin, Turkey

ARTICLE INFO

Keywords:
Ductility
Flexural behaviour
Finite element analysis
Lap-spliced bars
Steel fibre

ABSTRACT

The ductility of reinforced concrete (RC) beams is a prominent factor associated with their failure mode. In addition, different parameters affect the ductility and behaviour of steel fibres (SF) reinforced RC beams such as lap-splice length, longitudinal rebars ratio and SF content. This study intends to assess the influence of these parameters on the flexural behaviour and ductility of beams with lap-spliced bars. This study was performed in two steps. In the first one, 16 RC beams with a cross-section 150 mm wide and 200 mm high, and a length of 2300 mm with different lap-splice length were produced and the influence of SF content and lap-splice length on the flexural performance of specimens was studied. The specimens were tested under a four-point setup. One specimen was selected as a control without SF and lap-spliced bars. SF were added at three contents in terms of volume: 0%, 1% and 2%. In addition, six different lap-splice lengths were provided: l_d, 0.9l_d, 0.8l_d, 0.7l_d and 0.6l_d where l_d denotes the design lap-splice length. In the second step, a finite element software, ABAQUS, was employed to assess the effect of longitudinal rebars ratio and concrete compressive of concrete on the performance and ductility of SF-reinforced RC beams with lap-spliced bars. A novel simulation was used to model the bond-slip of rebars in concrete beams with lap-spliced bars and the results were compared with the case when bond-slip is neglected. The results showed that the lap-splice length could be decreased by 40%, relative to the design lap-splice length, when 2% SF were added and the transverse reinforcement spacing along the splice length was halved. In addition, the bond-slip performance of tensile rebars could be accurately simulated in both plain and SFRC beams while, when more than 1% SF were added, the slip between the tensile rebar and concrete could be neglected due to high reduction in slip as a result of adding SF.

1. Introduction

Deficiencies and shortcomings of concrete and steel, as the most widely used building materials, have led researchers to adopt new construction approaches. For instance, concrete's tensile response and its limitation in hazardous environments, along with steel's low performance against corrosion and its high unit weight, are among the main issues that should be addressed in the design and construction of concrete structures [1]. The use of steel fibre-reinforced concrete (SFRC) improves the ductile behaviour, the structural strength during transient load cycles, and the post-cracking tensile capacity of various structures [2-4]. The relatively low volume ratio of steel fibres (SF), usually limited to less than 2%, offers a limited improvement, which is comparable to conventional concrete prior to crack propagation [5]. On the other hand,

Abbreviations: A_t, transverse reinforcement area; C_x, side concrete cover; C_y, bottom concrete cover; C_s, free spacing between lap-spliced bars; d_t, elastic failure cracking factor; f_c', compressive strength of concrete; d_b, diameter of rebars; f_S, tensile stress of rebars; f_y, yield strength of rebars; i, ductility ratio; LVDT, linear variable differential transformer; l_d, design lap-splice length; PPF, polypropylene fibres; RC, reinforced concrete; R, projected rib area normal to bar axis/(normal bar perimeter × centre-to-centre rib spacing); S, transverse reinforcement spacing; SF, steel fibres; SFRC, steel fibre-reinforced concrete; ρ_{max}, maximum reinforcement ratio; ρ, reinforcement ratio; $\Delta_{0.85}$, displacement corresponding to 85% of the beam's maximum bending capacity; Δ_y, displacement corresponding to the beam's maximum bending capacity; τ_b, bond stress; τ_f, maximum bond stress.

* Corresponding author.
E-mail addresses: akarimipour@miners.utep.edu (A. Karimipour), jb@civil.ist.utl.pt (J. de Brito), ogencel@bartin.edu.tr (O. Gencel).

https://doi.org/10.1016/j.engstruct.2021.113362
Received 18 June 2021; Received in revised form 14 September 2021; Accepted 12 October 2021
Available online 21 October 2021
0141-0296/

after cracking, the presence of SF bridges the crack surfaces and improves the tensile capacity and ductility in contrast to the brittle behaviour of conventional concrete. This advantageous response of SF is mainly governed by the developed bond between fibres and concrete, the strength characteristics of the fibres and the effective distribution of fibres along the cracks [6,7]. Incorporating an ample amount of SF leads to a considerable tensile strength of concrete [8]. Additionally, SF enhances the SFRC members' toughness against cracking, improves the strain-hardening response of concrete prior to cracking, and increases energy absorption [9,10]. Furthermore, the application of SF enhances concrete's resistance when subjected to shear and torsion loads [11,17].

To further investigate the performance of SFRC beams, Li et al.[17] studied the effect of SF's volume fraction, aspect ratio and fibre type on the flexural strength of SFRC beams subjected to four-point bending tests. Four volume fractions (0.5 %, 1%, 1.5%, and 2%), three types of SF (straight, hooked-end, and corrugated) with 40, 60 and 80 aspect ratios were used. Consequently, the ultimate flexural capacity of SFRC beams was enhanced by 74.3%, 165%, and 112.7% compared to plain concrete with the use of straight, hooked-end, and corrugated SF, respectively. Moreover, the use of hooked-end SFRC beams provides the best flexural response compared to other types of fibres. Biolzi and Cattaneo [18] examined the shear and flexural behaviour of SFRC beams using a four-point bending test. The effect of SF on failure mechanism, ductility, initial cracking and crack patterns of the beams was also investigated. Adjusted beam's shear reinforcement system (SF, stirrup, none), various ratios of shear span effective depth (1.5, 2.5 and 3.5), and concrete's compressive strength were regarded as the main factors in the analysis. Following the experiments, they concluded that incorporating SF significantly contributed to enhancing the shear and flexural capacity and ductility of SFRC beams. The structural response of SFRC beams under transient load cycles was investigated to further evaluate the effect of incorporating SF in RC beams. Lee et al. [19] studied the structural behaviour of SFRC beams subjected to different loading rates. Different volume fractions of end-hooked SF were used to manufacture SFRC beams that were tested by applying blast, impact and quasi-static loading rates. Based on their study, the inclusion of SF improved beams' resistance to these loading conditions and increased energy absorption and load-bearing capacities. Furthermore, the incorporation of SF decreased the residual and maximum displacement. The authors also emphasized the fact that including low volume ratios of SF (i.e. 0.5% and 1%) cannot significantly prevent beams' brittle shear failure in the absence of stirrups. However, the use of stirrups considerably improves the ductility of the RC beam with similar high percentages of SF. They reported that the use of stirrups with 0.5% volume fractions provided the maximum strain rate for the SFRC beam. As another effort to investigate the performance of SFRC beams subjected to cyclic loading, Ranjbaran et al. [20] conducted an experimental study by testing seven full-scale specimens subjected to a four-point bending test. In addition to a control specimen in the absence of SF, six other specimens with 1%, 2%, and 4% SF contents in terms of volume were tested. Based on the acquired results, they stated that using SF at a minimum of 2% volume ratio enhanced the cyclic response of SFRC beams in addition to improving the flexural and shear strengths and the ultimate displacement. In another study, Roesler et al. [21] evaluated the critical responses of SFRC members. A total of 20 beams with various SF contents were produced and tested. In addition, 10 different longitudinal reinforcement ratios ranging from 0.2% to 2.5% were used in order to assess the influence of longitudinal rebar content. They found that the incorporation of SF led to a ductile performance with higher load-bearing capacity and lower cracks width. Soutsos et al. [22] investigated the flexural responses of SFRC beams under static and dynamic loads. Results of their study showed that the improvement influence of SF on the flexural responses of RC beams was higher than in specimens tested under a dynamic load.

Recently, improving the shear and flexural performance of RC beams with lap-spliced rebars has been tried and many investigations were done to measure the critical response of RC beams with lap-spliced bars. These bars affect the bond stress distribution between concrete and the longitudinal tension rebars and so that the flexural response of RC beams considerably declined with a brittle failure if sufficient lap-splice length is not provided to the bars. According to existing literature, the influence of admixtures, compressive strength of concrete and rib properties of the reinforcements was also studied [23]. Moreover, different phenomena such as corrosion in longitudinal rebars reduce the bond resistance between concrete and rebars, which is one of the main sudden failures in RC beams, particularly when a lap-spliced is created in the longitudinal tensile rebars [24]. In addition, many studies resulted in new analytical and experiential models to predict the bond strength of rebars in RC beams [25-28]. Conversely, the deformation and ductility of RC beams with lap-spliced rebars is an important matter that has attracted the attention of engineers in recent decades. Azizinamini et al. [29] measured the efficiency of ACI 318–14 [30] to estimate the adequate lap-splice length in RC beams to provide an appropriate ductility. They found that providing enough shear rebars over the lap-spliced bars plays an important role in order to offer adequate ductility of RC beams by increasing the bond resistance. Presently, a few investigations have been conducted to improve the bond resistance of rebars in RC beams with lap-spliced bars [31]. In this context, Ghalehnovi et al. [32] used SF to improve the structural performance and ductility of RC beams with lap-spliced bars subjected to cyclic loads. They tested a total of 10 RC beams reinforced with various lap-splice lengths by incorporating 0%, 1% and 2% SF in terms of volume. In addition to a control specimen, six SFRC beams were subjected to cyclic load application and the remaining specimens were tested by applying a static load. By evaluating the flexural capacity, dissipated energy, ductility and displacement of SFRC beams, they asserted that, in the specimens with 2% SF, the required lap-splice length can be reduced by 20% without an adverse effect on ductility and flexural capacity of beams.

As a continuous effort, Karimipour et al. [33] examined the effect of SF and polypropylene fibres (PPF) on the structural response of RC beams with lap-spliced bars and recycled aggregates. In this experimental approach, 40 specimens were prepared and subjected to a four-point bending test. PPF and SF were separately used at 0%, 1% and 2% in terms of volume to enhance the bond resistance between concrete and steel bars and increase the specimens' flexural capacity. Stiffness, ultimate deformation, load-bearing capacity and ductility of beams were monitored during the experiments. They concluded that the lap-splice length can be decreased by 40% without reducing the beam's flexural strength by adding 2% of SF or PPF in addition to using 100% recycled aggregate. In the design of RC beams, an ample amount of ductility by maintaining the reinforcement ratio is required to prevent sudden failure in RC beams and increase the warning time of the potential collapse. In this context, the bond between the reinforcement and concrete is one of the most notable parameters in the design procedure of RC beams with lap-spliced bars [34]. The efficacy of the lap-spliced bonding is governed by diameter and embedment length of reinforcement, the reinforcement ratio along the compressive strength of concrete and concrete cover [35]. Increasing confinement using transverse reinforcement along the lap-splice length prevents the occurrence of splitting cracks and minimizes cracks' width. It also improves the flexural capacity of RC beams by enhancing the bond strength between reinforcement and concrete [36]. In RC beams, the reinforcement ratio (ρ) should be less than the maximum value of the reinforcement ratio ρ_{max} [37]. In this regard, Rezaiee-Pajand et al. [38] proposed an accurate model to determine sufficient lap-splice length and required transverse reinforcement over the lap-spliced bars. The results showed that their model, with high agreement with the experimental results, could be used as a useful tool to provide adequate lap-splice length to guarantee the ductility of RC beams. In addition, they showed that the model proposed by Esfahani and Kianoush [39] had very low agreement with the experimental results and that it is not a suitable tool to estimate the adequate lap-splice length of bars and the transverse reinforcement

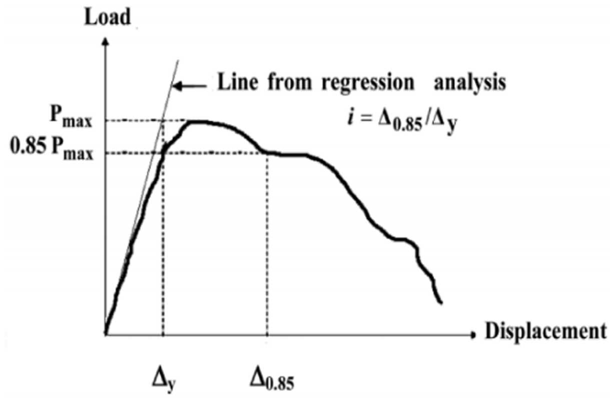

Fig. 1. Determination of the shape of the RC beam.

spacing in RC beams.

All previous studies found that providing sufficient lap-splice length to offer an adequate ductility of RC is an important factor that should be considered in designing RC beams with lap-spliced bars. For this purpose, Cohen and Bertolt [40] presented the load–displacement relationship in an attempt to assess the ductility of the RC beams, as shown in Fig. 1. They proposed the ductility index (i) as the ratio of displacement corresponding to 85% of the beam's maximum bending capacity ($\Delta_{0.85}$) to the displacement corresponding to the beam's maximum bending capacity (Δ_y), as presented by Eq. (1).

$$i = \frac{\Delta_{0.85}}{\Delta_y} \quad (1)$$

2. Calculation of the lap-splice length

In the present study, the lap-splice length was calculated according to Rezaiee-Pajand et al. [38] research, which is in good agreement with the experimental results. In this regard, the lap-splice length can be calculated using Eq. (2).

$$l_d = \frac{f_S d_b}{a\sqrt{f_c^{'}} - 3.23} \quad (2)$$

where d_b and $f_S, f_c^{'}$ are the diameter and tensile stress of the longitudinal tensile reinforcement and compressive strength of concrete, respectively. In addition, a is a modification factor and calculated according to reference [34].

3. Research significance

The literature reported that a minimum lap-splice length should be provided in RC beams to offer an adequate load-bearing capacity and ductility [10-25]. Bond resistance is the main parameter affecting the design lap-splice length [38]. Additionally, previous studies showed that fibres significantly improve the bond resistance between concrete and rebars. However, only a few limited studies have assessed the influence of limited content of fibres on the flexural performance of RC beams with lap-spliced bars [33,34]. However, there are more variables influencing the flexural performance of SFRC beams with lap-splice bars that have not been assessed so far including the transverse reinforcement spacing along the splice bars and longitudinal tensile rebars ratio. Therefore, in this study, the effect of different variables including the SF content, lap-splice length, longitudinal rebars ratio and transverse reinforcement spacing on the flexural responses and ductility of RC beams was studied. Additionally, in terms of numerical evaluation of the structural performance of RC member, slip between concrete and the rebars is neglected, which is very important factor when there are spliced bars and SF-reinforced concrete is used. Because. Existing software is unable to simulate fibres distribution in the concrete matrix. Therefore, this study is the first investigation that developed a new finite element simulation for bond-slip behaviour of rebars in SF-reinforced concrete with connectors that play a spring role to model the exact slip between concrete and the rebars in SF-reinforced concrete and high accurate simulation of SFRC beams with lap-spliced bars, because slip between the tensile rebars and concrete in the splice region is an important parameter affecting the flexural performance and ductility of RC beams.

Fig. 2. SF with hooked ends.

Table 1
Concrete mixes design.

Specimen	Water (kg/m^3)	Cement (kg/m^3)	NCA (kg/m^3)	NFA (kg/m^3)	SF (kg/m^3)
0% SF	165	40[illegible]	8[illegible]	950	0
1% SF	165	400	76[illegible]	950	78
2% SF	165	400	68[illegible]	950	156

Fig. 3. Direct tensile test setup.

4. Specimen specifications

4.1. Specifications of SF

To produce fibre-reinforced concrete, SF with hooked ends were used, as shown in Fig. 2. The modulus of elasticity, tensile strength and failure strain of fibres are 200 GPa, 2 GPa and 3%, respectively. In addition, the length and equivalent diameter of SF are 60 mm and 0.9 ± 0.03, respectively.

Table 2
Rebars test results

Rebars diameter (mm)	Yield strength (MPa)	Ultimate strength (MPa)	Yield strain (%)	Ultimate strain (%)	Modulus of elasticity (GPa)
8	371	508.49	0.1610	24.51	203.74
10	375	554.24	0.1667	27.14	222.65
20	408	677.99	0.2435	25.51	210.11

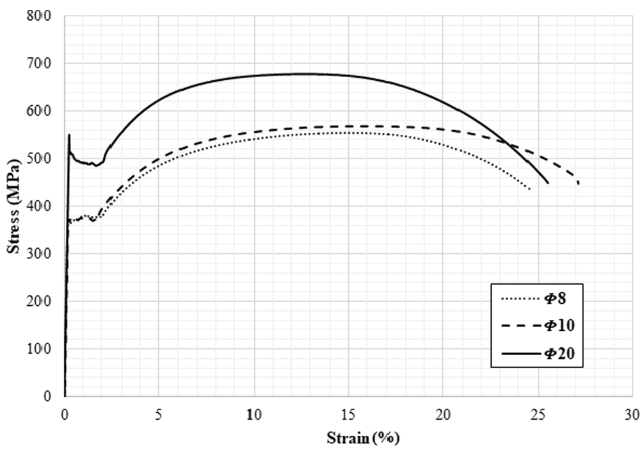

Fig. 4. Strain-stress curve of the tensile reinforcement.

Table 3
Compressive and splitting tensile strengths of the concrete samples.

	Compressive strength (MPa)		Splitting tensile strength (MPa)	
	Average value	Coefficient of variation	Average value	Coefficient of variation
Control	35.3	1.3	3.26	[illegible]
l_d-0%	33.6	3.6	3.17	[illegible]
l_d-1%	37.7	1.7	6.60	0.3
l_d-2%	39.3	1.2	7.43	0.7
0.9l_d-0%	34.3	1.3	3.13	0.17
0.9l_d-1%	37.3	1.2	6.76	[illegible]
0.9l_d-2%	40.3	0.7	7.30	0.3
0.8l_d-0%	33.0	1.0	[illegible]	0.1
0.8l_d-1%	38.7	0.2	6.40	0.1
0.8l_d-2%	40.3	0.6	[illegible]	0.3
0.7l_d-0%	33.3	[illegible]	3.23	0.7
0.7l_d-1%	37.7	1.3	6.53	0.2
0.7l_d-2%	39.7	0.4	7.40	0.2
0.6l_d-0%	33.3	1.7	3.33	0.1
0.6l_d-1%	38.0	1.2	6.37	0.3
0.6l_d-2%	40.3	0.5	7.43	0.1

4.2. Concrete mixes

To manufacture the concrete specimens, cement was mixed with gravel, sand and fibres (at 0%, 1% and 2%) and then a solution of water and high-performance superplasticizer was added until the steel fibres were uniformly distributed in the concrete matrix. The concrete mix compositions are represented in Table 1. It should be mentioned that the total water/cement ratio of all samples was kept constant at 0.41.

4.3. Steel rebars

Rebars with diameters of 20 mm, 10 mm and 8 mm were used as tensile, compressive and transverse reinforcement, respectively. The installed rebars are identical in all the specimens and the compressive and tensile bar areas are 157 mm^2 and 628 mm^2, respectively. According to Fig. 3, rebars were subjected to direct tension tests and their specifications were measured. The results are presented in Table 2. In addition, Fig. 4 presents the strain–stress curve rebars obtained using the direct tensile test.

4.4. Concrete properties

The compressive and splitting tensile strengths of concrete mixes were measured at 28 days after curing. To measure the strengths of the specimens, the average strength values of three 150 mm × 300 mm cylindrical specimens were produced from the mix of each specimen and then subjected to compressive and splitting tensile loading conditions were recorded. The concrete tensile and compressive strength has been determined according to C496/C496M, BS EN 12390–1, 2 and 3 [39-43] Table 3 summarizes the reported compressive and splitting tensile strengths of the tested specimens. Where, l_d is the lap-splice length calculated using Eq. (2) and 1% is the SF content in terms of volume percentage. Regarding Table 3, the use of SF increased both the compressive and splitting tensile strengths of concrete due to the bridging role of fibres, which keep particles together and transfers stress along the cracking. There, the compressive strength of concrete mixes was improved by an average of 8.2% and 14.3% when 1% and 2% SF were added, respectively. Additionally, adding 1% and 2% SF improved the splitting tensile strength of concrete mixes of specimens by an average of 8[illegible]% and 96%, respectively. Additionally, as shown in Table 3, there is a slight difference between the compressive and splitting tensile strengths of the same concrete mix for different specimens. For example, the average compressive strength of control specimens, l_d-0%, 0.9l_d-0%, 0.8l_d-0%, 0.7l_d-0% and 0.6l_d-0% are 35.3, 33.6, 34.3, 33.0, 33.3 and 33.3 MPa. This slight difference could be attributed to the laboratory technician error, setup error and curing condition that are normal in lab testing. The influence of fibres on the compressive and splitting tensile strengths of concrete was studied by Karimipour and de Brito in detail [23]. In addition, the distances from the extreme tension and compression fibres were 162 and 25 mm, respectively. Furthermore, the compressive stress–strain relationship of concrete with different SF contents are presented in Fig. 5. To measure the stress–strain relationship of concrete, three 150 mm × 300 mm cylindrical specimens were produced from each mix (plain and SF-reinforced concrete) and then positioned in a single ring that involved a strain gauge with the accuracy of 0.001 mm according to ASTM C469 [45], as illustrated in Fig. 6. The same observation was reported by Ran et al. [46] that confirms the presented stress–strain relationship of concrete samples. Then, the stress–strain relationship of specimens was recorded with the use of a computer. It should be stated that these results are necessary to consider as input variables for the numerical section of this study.

Regarding Fig. 5, with the addition of SF, the ultimate axial stress of concrete significantly increased and the axial stress further increased for higher SF contents. By increasing the applied load, cracks occurred on the external surface of the unreinforced concrete samples, then widened and, eventually, the specimen's rapture can occur in the hardening zone. Increasing the percentage of SF improved the resistance against failure, and that increased the strain of concrete. In addition, the tensile stress–strain relationship of concrete samples was measured according to the study of Al-Osta et al [47] for different SF contents. The results are illustrated in Fig. 7. Regarding this figure, it can be seen that, at the elastic stage, the stress–strain relationship was linear until the tensile stress reached a certain peak due to the bridging role of SF, which transfers stress along cracks and corresponded to the appearance of the first crack. After that, the tensile stress dropped abruptly and then gradually decreased as the tensile strain continued to increase due to increasing the slip between fibres and concrete. In most of the FRC specimens, the tensile stress, after dropping abruptly upon first cracking, gradually decreased as the tensile strain increased. However, in some of

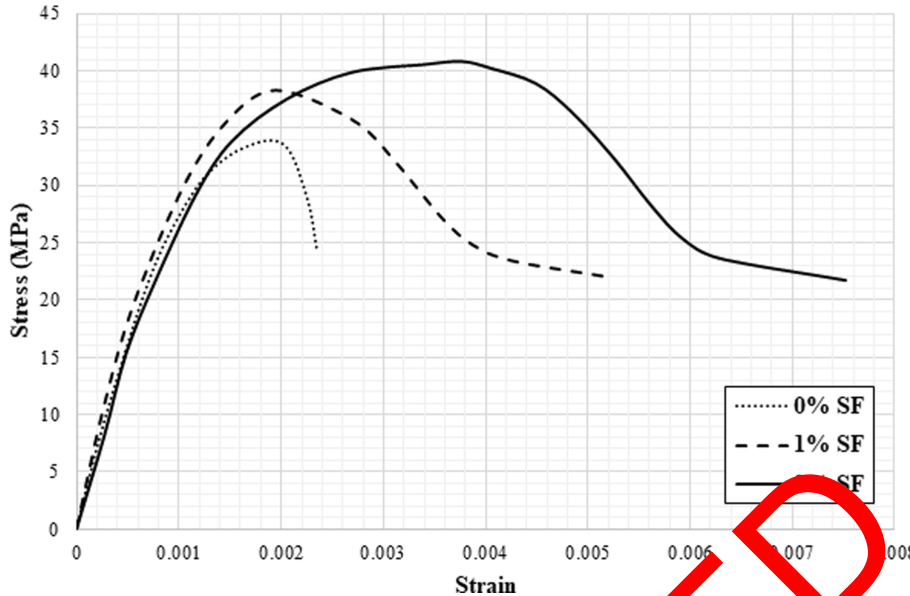

Fig. 5. Compressive stress–strain behaviour of concrete with different SF content.

Fig. 6. Stress–strain relationship of the concrete test setup.

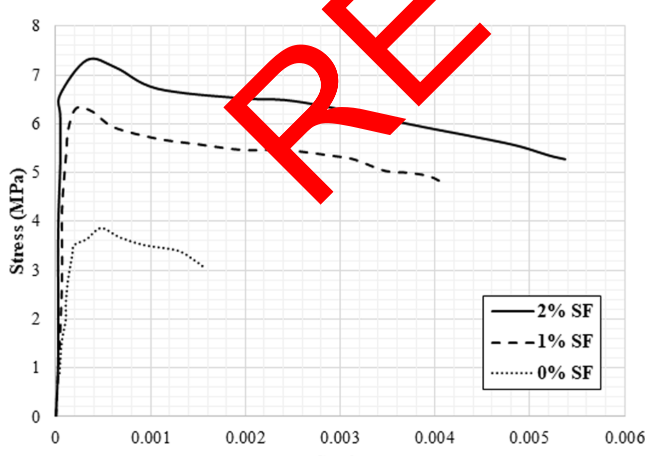

Fig 7. Tensile stress–strain behaviour of concrete with different SF content.

the SFRC, the tensile stress, after dropping abruptly upon first cracking, gradually increased to an even higher peak than the first cracking strength as the tensile strain increased, and thus exhibited strain hardening behaviour. More details about the tensile stress–strain

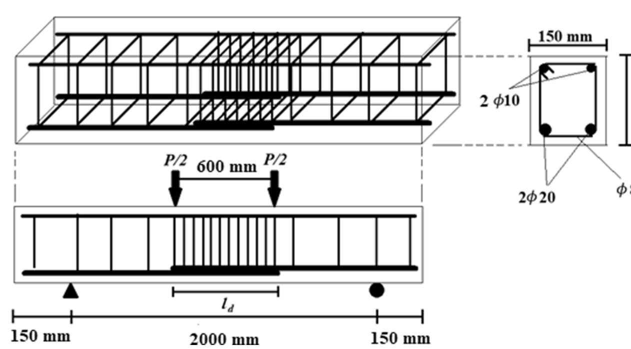

Fig. 8. Geometry of the specimens and rebars layout.

relationship of SF content could be also found in the study performed by Kwan and Chu [48].

4.5. Geometrical properties of the concrete specimens

In this study, a total number of 16 RC beams with height, width and length of 200, 150, and 2300 mm, respectively were prepared using different SF contents. Five lap-splice lengths were considered: l_d, $0.9l_d$, $0.8l_d$, $0.7l_d$ and $0.6l_d$ where l_d denotes the sufficient calculated lap-splice

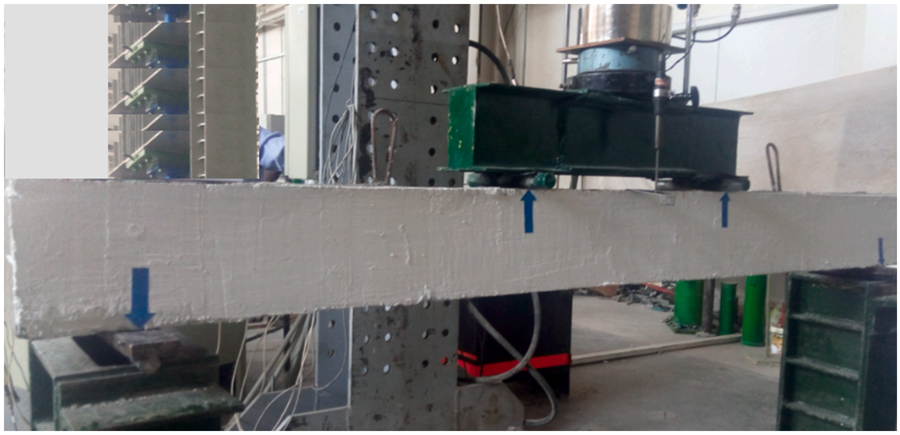

Fig. 9. Four-point flexural test setup.

length. One specimen was considered as a control without lap-splice bar and SF. Fig. 8 shows the geometrical properties and layout of the longitudinal and transverse rebars. It should be noted that the longitudinal rebars ratio for the control specimen and those with lap-spliced bars is constant.

5. Test setup and loading conditions

Specimens were tested under a four-point bending setup at 28 days after curing, as shown in Fig. 9. The purpose of this test was to determine the flexural performance and ductility of beams with lap-spliced bars. The tested beam with a 2000 mm span had two simple supports and was subjected to axial load with 600 mm eccentric distance. One specimen was selected as the control. During the text procedure, displacement was constantly monitored and loading remained up to the specimen's failure. To perform a load, 500 kN capacity load-cell was used and load applied at 5 mm/min rate. The deflection of the beam was recorded with a Linear Variable Differential Transformer (LVDT) with the accuracy of 0.001 mm, placed at the mid-span under the specimen.

6. Experimental results

6.1. Load-displacement behaviour

In this section, the load–displacement behaviour of the specimens was studied. The results are presented in Fig. 10. As per Fig. 10a, there is a difference between the control specimens and that with adequate lap-splice length (l_d), which shows the design lap-splice length is enough. Additionally, adding SF significantly improved both the load-bearing capacity and mid-span displacement of specimens when the design lap-splice length (l_d) was provided and the performance of the beam was further improved with increasing SF content. Additionally, adding SF delays the crack initiation and acts after the cracks appear which led to increasing the deformation after the maximum load-bearing capacity with no significant reduction in load capability when a sufficient lap-splice length was provided (Fig. 10a).

Conversely, reducing the lap-splice length led to reducing both the maximum load-bearing capacity and the deformation of the beams while adding SF improved the performance of beams with reduced lap-splice length. According to Fig. 10b, reducing the lap-splice length by 10% without SF slightly declined the maximum mid-span displacement of the beam. Reducing the lap-splice length by more than 10% ($0.9l_d$) substantially declined the maximum strength and deformation of the specimens. However, with the use of SF, the lap-splice length could decrease by 20% with no reduction in the maximum load-bearing capacity of RC beams with lap-spliced bars (Fig. 10c). This could be attributed to the improvement of the bond resistance of tensile rebars in the beam when fibres are used. In addition, the bridging effect of SF played an effective role in reducing the cracks width through the specimens and around the rebars, which led to increasing the confinement effect around the rebars. In addition, there is a slight difference between the maximum strength and deformation of the control specimen and those of the specimen with a $0.7l_d$ lap-splice length when 2% SF were added (Fig. 10d). Conversely, adding SF did not affect the structural performance of specimens when the lap-splice length declined by 40% ($0.6l_d$) as shown in Fig. 10e.

Furthermore, the influence of lap-splice length on the flexural strength of specimens was measured considering the SF content constant. The results are presented in Fig. 11. Regarding Fig. 11a, there is no significant difference between the load-bearing capacity and deformation of the control specimen and that produced with sufficient lap-splice length (l_d). On the other hand, the reduction in lap-splice length without SF decreased the maximum resistance and deformation of RC beams due to increasing the slip between the longitudinal tensile rebars and concrete. Therefore, a sudden reduction in load-bearing capacity was observed after a maximum load-bearing capacity of beams when more than 10% lap-splice length decreased. Conversely, adding 1% SF led to improving the load-bearing capacity and deformation, and the lap-splice length could decrease by 20% with no reduction in flexural strength of RC beams. This could be attributed to increasing bond resistance and reducing slip between longitudinal tensile rebars and concrete. However, the addition of 1% SF did not significantly affect the load–displacement relationship of RC beams when the lap-splice length decreased by more than 20%. Furthermore, a significant improvement in load-deformation behaviour of RC beams with up to 20% reduction in lap-splice length was observed when 2% SFF were added (Fig. 11c). Additionally, there is no substantial difference between the control specimens and that having $0.7l_d$ in terms of maximum displacement and load-bearing capacity. However, a 40% reduction in lap-splice length substantially decreased the flexural behaviour of RC beams whereas 2% SF were added. Furthermore, the changing trend in maximum mid-span displacement and load-bearing capacity of the specimens, and their values are presented in Figs. 12 and 13.

The lap-splice length could be cut by 20% when 2% SF were used with no reduction in strength and deformation of the beams. Conversely, reducing the lap-splice length by 30% in 2% SFRC beams substantially decreased the mid-span displacement; however, the ultimate strength slightly dropped. Therefore, the addition of 2% SF improved the maximum load-bearing capacity of specimens with l_d, $0.9l_d$ and $0.8l_d$ lap-splice length by 25%, 12.5% and 11%, respectively, relative to that control specimen without splice and SF. Additionally, the maximum displacement of specimens with l_d, $0.9l_d$ and $0.8l_d$ lap-splice length increased respectively by 22%, 13% and 3% when 2% SF were added. Conversely, the maximum strength and displacement of the specimen

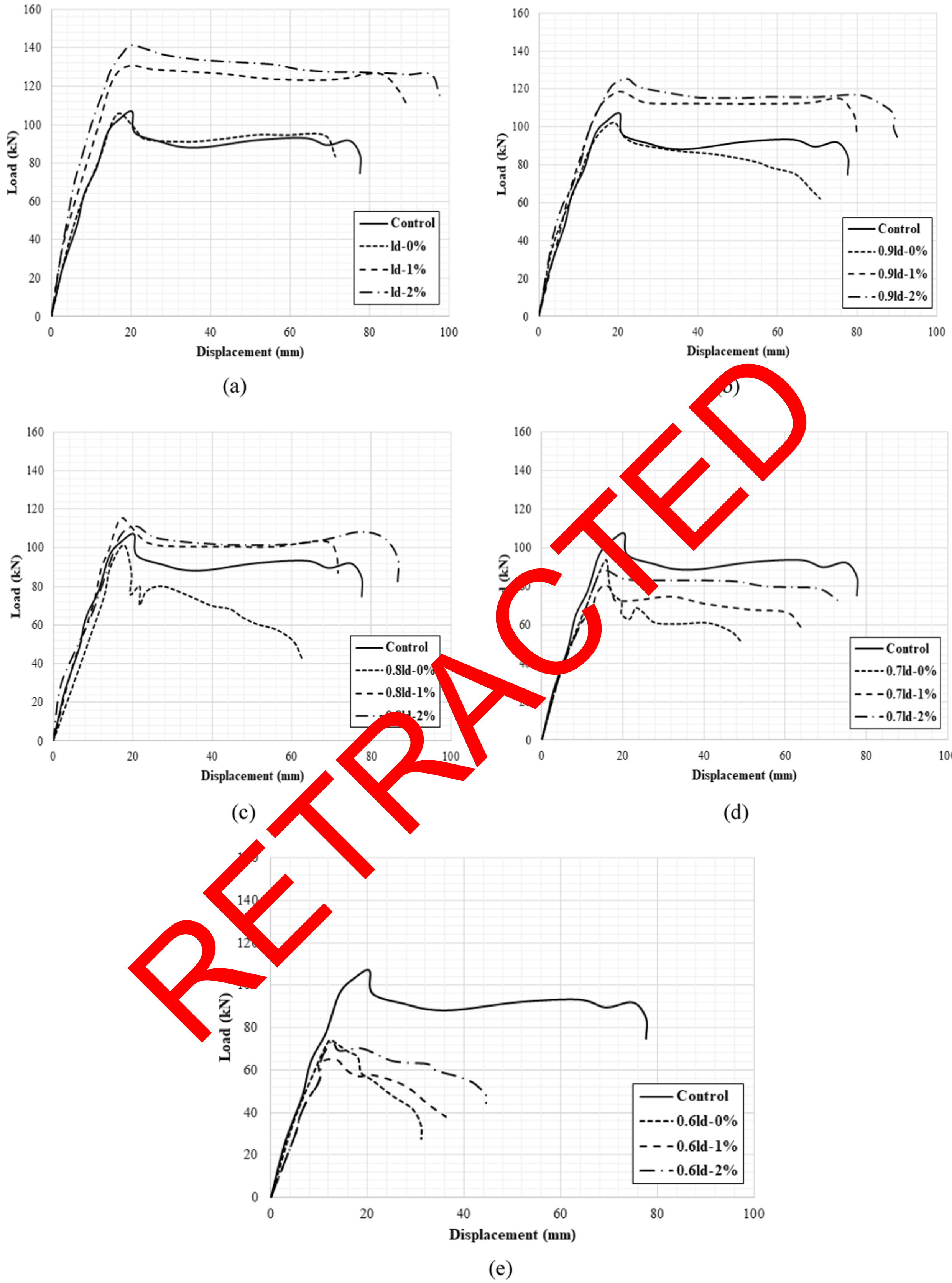

Fig. 10. Influence of SF content and lap-splice length on the load–displacement behaviour of specimens.

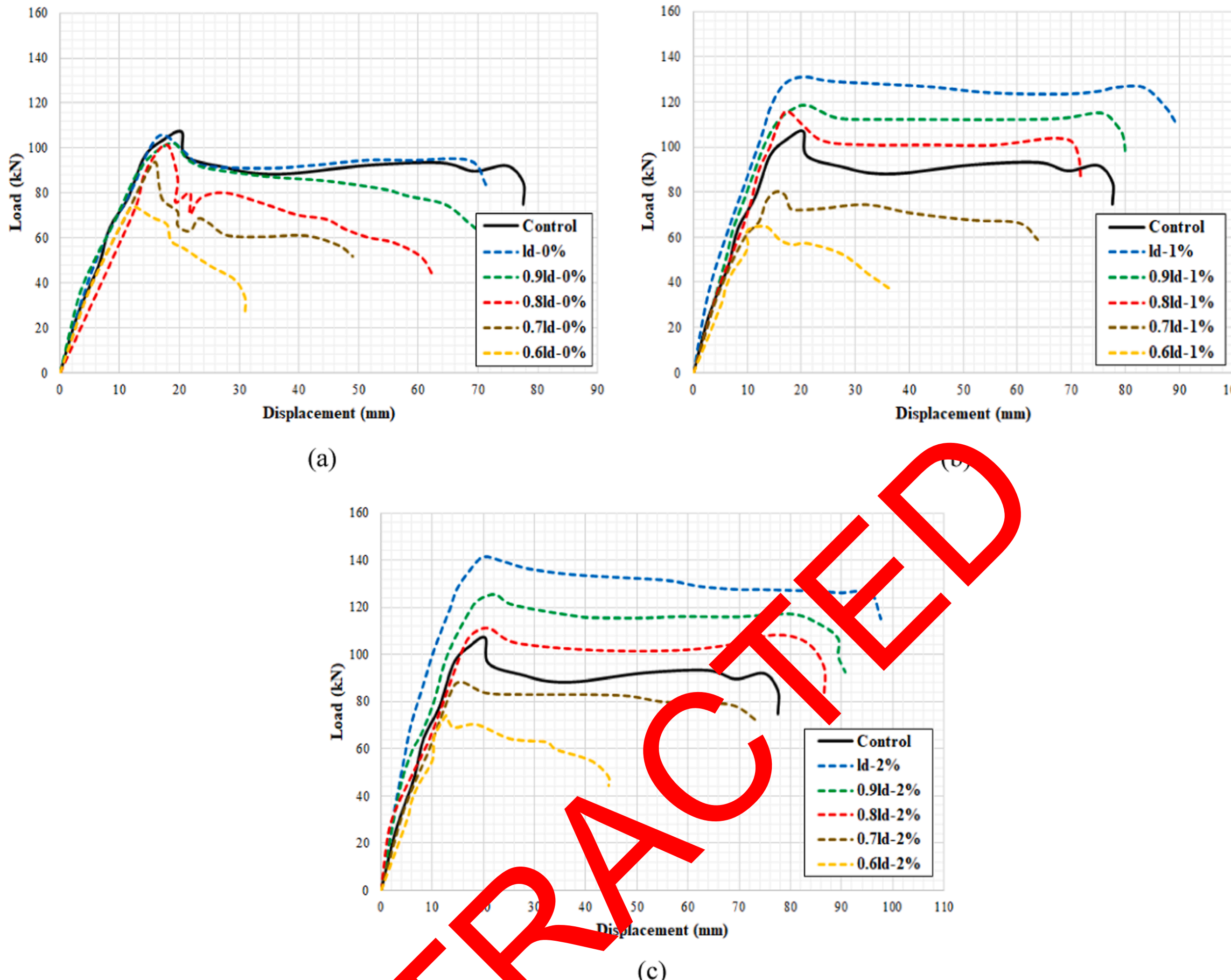

Fig. 11. Influence of lap-splice length on the load–displacement behaviour of specimens containing various SF contents: a) without SF, b) 1% SF and c) 2% SF.

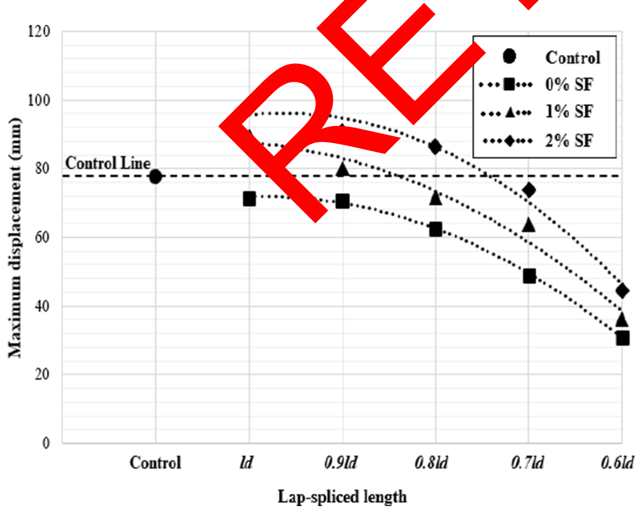

Fig. 12. Influence of SF content on the maximum mid-span displacement of specimens with different lap-splice lengths.

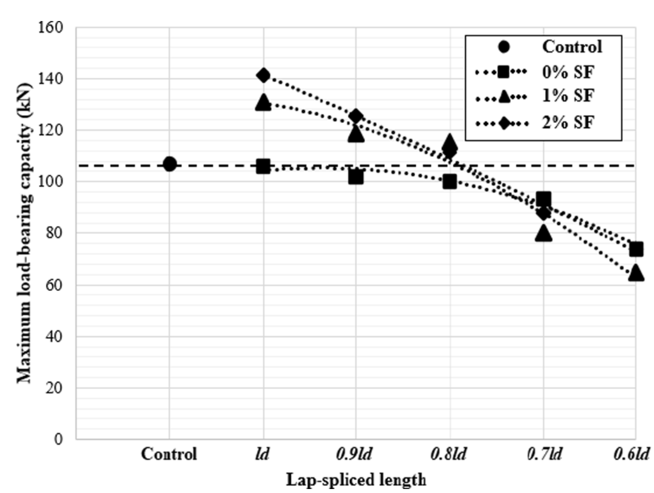

Fig. 13. Influence of SF content on the maximum load-bearing capacity of specimens with different lap-splice lengths.

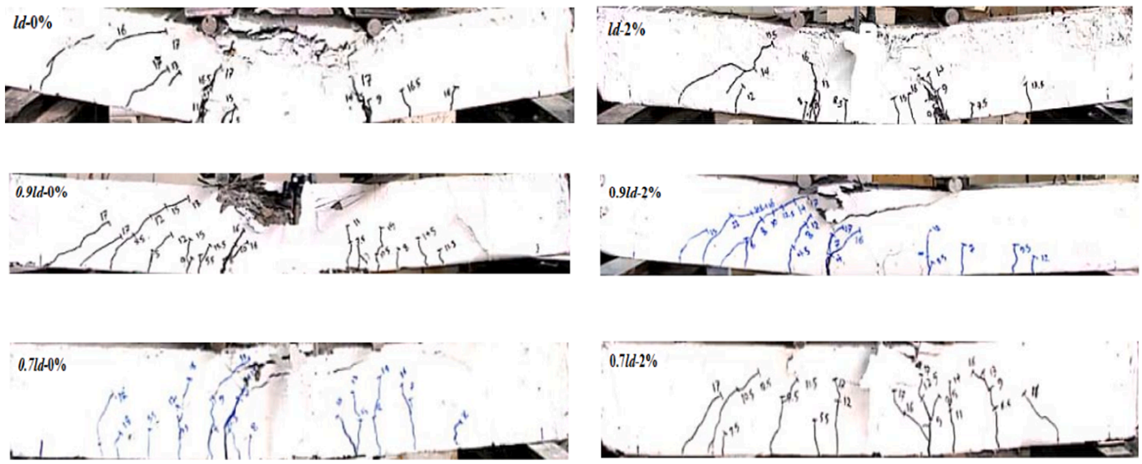

Fig. 14. Cracks propagation and failure mode of the specimens with lap-spliced bars during loading.

Table 4
Cracks width and load-bearing capacity of specimens

Specimen	Loading of first crack occurrence (kN)	Specimen's failure load (kN)	Initial cracks' width (mm)	Crack width at the peak load (mm)
Control	28.8	107.0	3.5	19.3
l_d-0%	25.5	105.8	3.1	11.6
l_d-1%	32.7	130.8	2.6	8.8
l_d-2%	36.6	141.3	2.2	6.6
0.9l_d-0%	22.5	102.1	5.0	27.5
0.9l_d-1%	29.7	118.6	3.8	20.9
0.9l_d-2%	32.4	125.4	2.9	16.0
0.8l_d-0%	20.1	100.3	5.9	32.5
0.8l_d-1%	28.9	115.6	4.5	24.[illegible]
0.8l_d-2%	29.6	118.3	3.4	18.7
0.7l_d-0%	18.2	80.1	6.5	35.8
0.7l_d-1%	21.1	88.5	5.0	27.[illegible]
0.7l_d-2%	23.4	93.6	3.7	2[illegible].4
0.6l_d-0%	14.2	64.8	[illegible].2	39.6
0.6l_d-1%	16.3	73.2	5.5	30.3
0.6l_d-2%	18.7	73.9	4.1	22.6

with 0.7l_d declined by 4% and 15% when 2% SF were added, respectively.

6.2. Modes of failure

Fig. 14 shows the failure and cracks distribution in typical specimens. Providing sufficient lap-splice length played an effective role in modes of failure and specimens with enough lap-splice length failed with large deformation. In addition, using SF decreased the cracks width and more cracks propagated by increasing SF content. By reducing the lap-splice length, specimens failed suddenly with low deformation. This is attributed to the large reduction in bond strength of the rebars over the spliced region. Therefore, cracks concentrated at the spliced region. On the other hand, since SF improved the bond resistance between the longitudinal rebars and concrete, specimens failed with more deformation and flexibility when 2% SF were added. In addition, both initial and failure crack width were measured using HFBTE CK-102 Digital Concrete Crack Width Gauge Meter, and the results are presented in Table 4.

There, the addition of SF decreased both the maximum and initial cracks width due to the bridging role of fibres and transferring the tensile stress along the cracks. Conversely, reducing the lap-splice length increased the width of the cracks and it substantially increased when the lap-splice length declined by 40%. In addition, SF did not significantly decrease the cracks width in specimens with 0.6l_d lap-splice length, which shows the importance of providing an adequate lap-splice length.

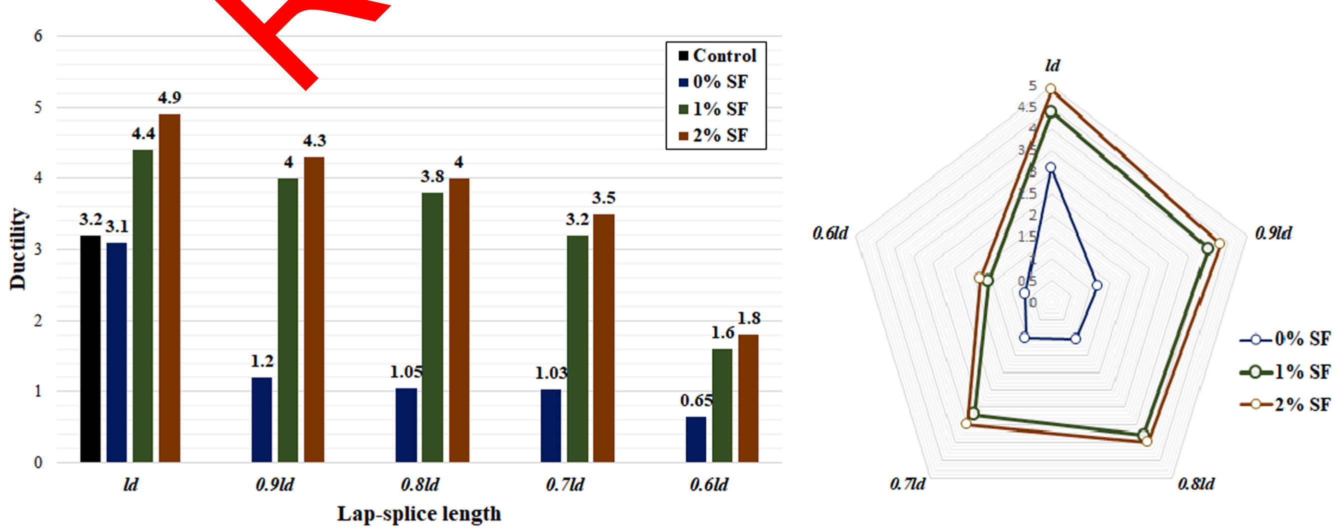

Fig. 15. Influence of SF on the ductility of the beam for different lap-splice lengths.

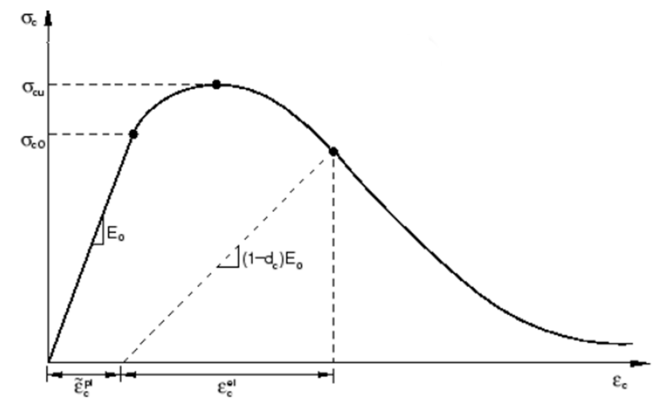

Fig. 16. Simulated response of concrete subjected to compression by finite element simulation.

6.3. Ductility

As mentioned above, the ductility and deformation of RC beams at the failure point are very important issues. In this section, the influence of SF on the ductility of RC beams with various lap-splice lengths was studied. The results are presented in Fig. 15.

There is no difference between the control specimens without lap-spliced bars and those reinforced with l_d. In addition, adding SF had a significant improvement influence on the ductility of specimens and ductility was further improved by increasing SF contents. However, adding SF did not significantly enhance the ductility of RC beams with $0.6l_d$. Therefore, specimens failed with deformation, which functions as an alarm to residents to leave the place under the beam. Without SF, the ductility of specimens considerably decreased when the lap-splice length declined: it dropped by 62.5%, 67.2%, 67.8% and 79.7% when the lap-splice length decreased by 10%, 20%, 30% and 40%, respectively. The lap-splice length could be cut by 30% $(0.7l_d)$ when 2% SF were added with no reduction in ductility.

7. Numerical results

In this section, the influence of various parameters, including transverse reinforcement spacing along the lap-spliced region and longitudinal tensile rebars ratio, on the flexural performance and ductility of SFRC beams with lap-spliced bars was numerically studied. For this aim, a new highly accurate model was developed in finite element method software, ABAQUS, by considering both slip and no-slip between the longitudinal tensile rebars and concrete, which is the main novelty of this study because there is no study to perform a bond-slip analysis between the rebars and concrete when SF were used. In addition, previous investigations have only measured the influence of limited SF contents and lap-splice lengths [26-28].

7.1. Materials' definition

The most important issue in numerical analysis is the accurate and exact definition of materials. Following the experimental results, SFRC beams with lap-spliced bars were adopted to the ABAQUS software as a finite element approach to analyse the effect of different main parameters on the critical responses of RC beams under flexure. To simulate the linear and nonlinear properties of concrete, the isotropic SOLID C3D8R element was used in the model. Nonlinear characteristics of concrete were considered to determine the concrete damage by finite element simulation. Concrete's failure was analysed by employing the generalized state of the Drucker-Prager's inner cone collapse criterion. Compressive strength, nonlinear strain, compression damage (d_c) and corresponding strain were analysed to determine the stress–strain response of concrete subjected to compression. In the numerical

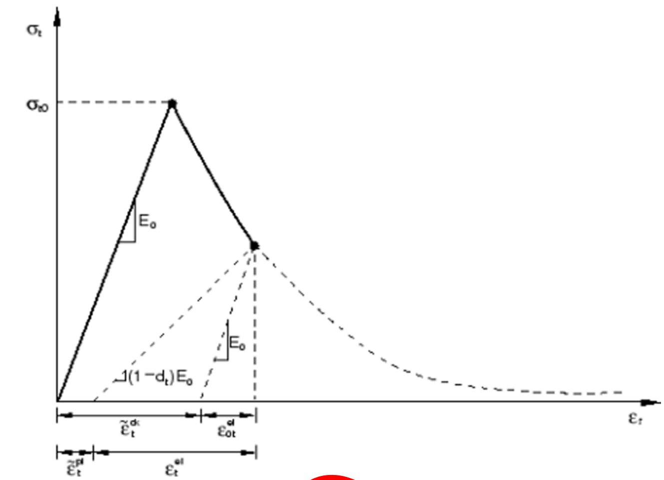

Fig. 17. Defined response of concrete subjected to tension in the finite element model.

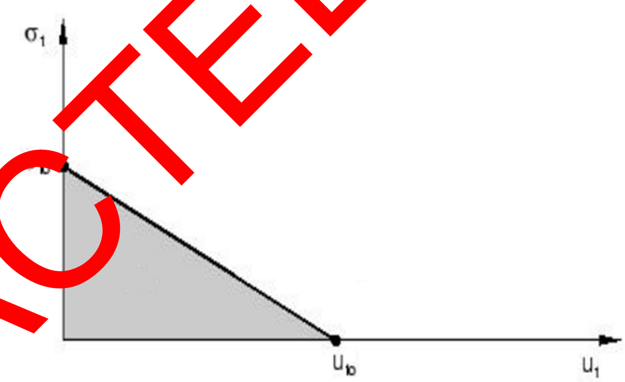

Fig. 18. Tensile response of concrete after cracking.

analyses, the real strain values were converted to a nonlinear strain using the following function, as illustrated in Fig. 16 [49]:

$$\bar{\varepsilon}_c^{in} = \varepsilon_c - \varepsilon_c^{cl} \tag{3}$$

Furthermore, the plastic strain values that correspond to the concrete's compressive strength were determined using the equation below [49]:

$$\bar{\varepsilon}_c^{pl} = \bar{\varepsilon}_c^{in} - \frac{d_c}{(1-d_c)}\frac{\sigma_c}{E_c} \tag{4}$$

The compression damage (d_c) is also calculated using the following proposed function:

$$d_c = 1 - \left[\frac{\frac{\sigma_c}{E_0}}{0.2\varepsilon_c^{in} + \frac{\sigma_c}{E_0}}\right] \tag{5}$$

Based on the experimental results, concrete's compressive and tensile strengths were simulated using the finite element model. To evaluate the stress–strain relationship of concrete subjected to tension, characteristics such as nonlinear strain, tensile damage and corresponding strain were considered and the actual strain was converted to the nonlinear strain. Fig. 17 shows the concrete's tensile strength using the finite element method. In this regard, the values of the strain of plastic corresponding to the tensile strength of the concrete at any given moment are determined by Eq. (6) [49].

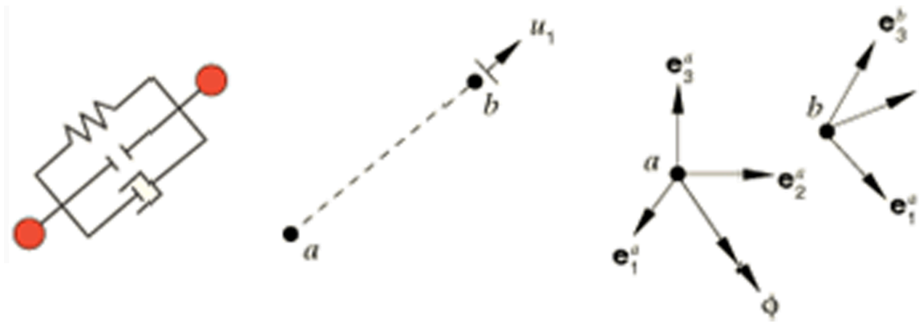

Fig. 19. Schematic of incorporated translator elements.

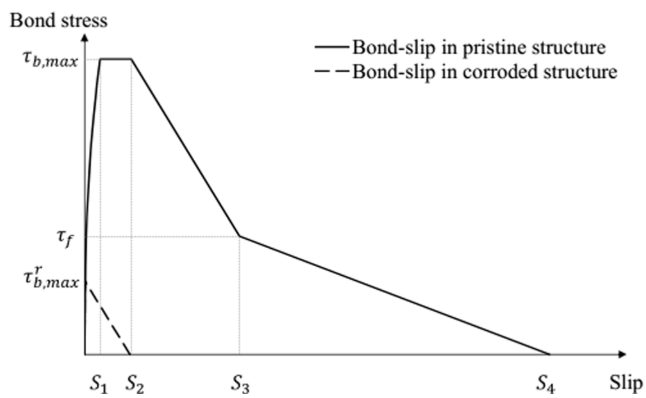

Fig. 20. Bond-slip response of ribbed bars.

$$\overline{\varepsilon}_c^{pl} = \overline{\varepsilon}_c^{in} - \frac{d_c}{(1-d_t)}\frac{\sigma_t}{E_c} \tag{6}$$

In which σ_t and E_c denote the tensile stress and modulus of elasticity, respectively. Plain concrete can transfer tension within the cracks. On the other hand, SFRC concrete is capable of carrying considerable tensile forces at each crack besides tension within cracks. Such an effect considerably enhances tension stiffening. Eq. (7) was used to determine the tensile strength of concrete after the occurrence of cracks. This linear response is illustrated in Fig. 18. The tensile behaviour of concrete after cracking should be considered as linear according to Kaw's study [49]. For this purpose, the following equation is proposed by Kaw [49], as shown in Fig. 18.

$$[\text{illegible}]_o = 2G_1/\sigma_{10} \tag{7}$$

Where G_1 is the area under the single line and d_t is elastic failure cracking factor, which is calculated as follows:

Table 5
Properties of the simulated specimens

Specimen	SF (%)	l_d (mm)	S (mm)	d_b (mm)	Specimen	SF (%)	l_d (mm)	S (mm)	d_b (mm)
l_d –0%-80–24	0	600	[illegible]	[illegible]	0.8l_d –1%-60–20	1	480	60	20
l_d –0%-80–20	0	600	80	20	0.8l_d –1%-40–24	1	480	40	24
l_d –0%-60–24	0	600	60	24	0.8l_d –1%-40–20	1	480	40	20
l_d –0%-60–20	0	[illegible]	60	20	0.6l_d –1%-80–24	1	360	80	24
l_d –0%-40–24	0	600	[illegible]	24	0.6l_d –1%-80–20	1	360	80	20
l_d –0%-40–20	0	600	40	20	0.6l_d –1%-60–24	1	360	60	24
0.8l_d –0%-80–24	0	480	80	24	0.6l_d –1%-60–20	1	360	60	20
0.8l_d –0%-80–20	0	[illegible]	80	20	0.6l_d –1%-40–24	1	360	40	24
0.8l_d –0%-60–24	0	480	60	24	0.6l_d –1%-40–20	1	360	40	20
0.8l_d –0%-60–20	0	480	60	20	l_d –2%-80–24	2	600	80	24
0.8l_d –0%-40–24	0	480	40	24	l_d –2%-80–20	2	600	80	20
0.8l_d –0%-40–20	0	480	40	20	l_d –2%-60–24	2	600	60	24
0.6l_d –0%-80–24	0	360	80	24	l_d –2%-60–20	2	600	60	20
0.6l_d –0%-80–20	0	360	80	20	l_d –2%-40–24	2	600	40	24
0.6l_d –0%-60–24	0	360	60	24	l_d –2%-40–20	2	600	40	20
0.6l_d –0%-60–20	0	360	60	20	0.8l_d –2%-80–24	2	480	80	24
0.6l_d –0%-40–24	0	360	40	24	0.8l_d –2%-80–20	2	480	80	20
0.6l_d –0%-40–20	0	360	40	20	0.8l_d –2%-60–24	2	480	60	24
l_d –1%-80–24	1	600	80	24	0.8l_d –2%-60–20	2	480	60	20
l_d –1%-80–20	1	600	80	20	0.8l_d –2%-40–24	2	480	40	24
l_d –1%-60–24	1	600	60	24	0.8l_d –2%-40–20	2	480	40	20
l_d –1%-60–20	1	600	60	20	0.6l_d –2%-80–24	2	360	80	24
l_d –1%-40–24	1	600	40	24	0.6l_d –2%-80–20	2	360	80	20
l_d –1%-40–20	1	600	40	20	0.6l_d –2%-60–24	2	360	60	24
0.8l_d –1%-80–24	1	480	80	24	0.6l_d –2%-60–20	2	360	60	20
0.8l_d –1%-80–20	1	480	80	20	0.6l_d –2%-40–24	2	360	40	24
0.8l_d –1%-60–24	1	480	60	24	0.6l_d –2%-40–20	2	360	40	20

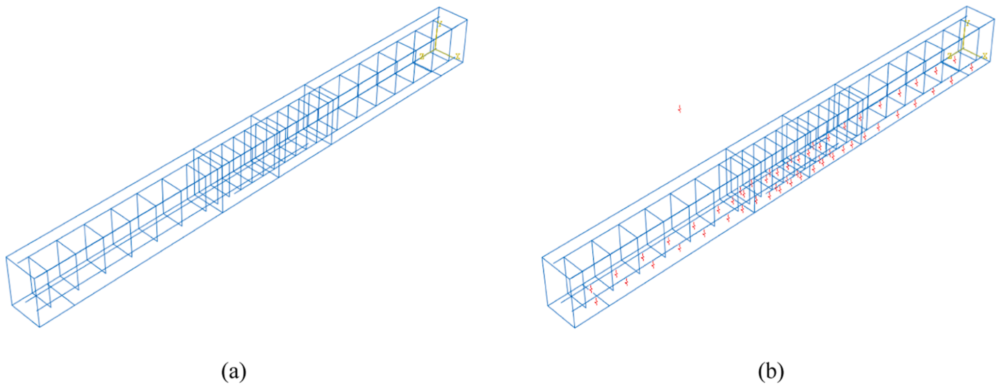

Fig. 21. Finite element simulation of specimens in ABAQUS a) without slip and b) with slip (using connector).

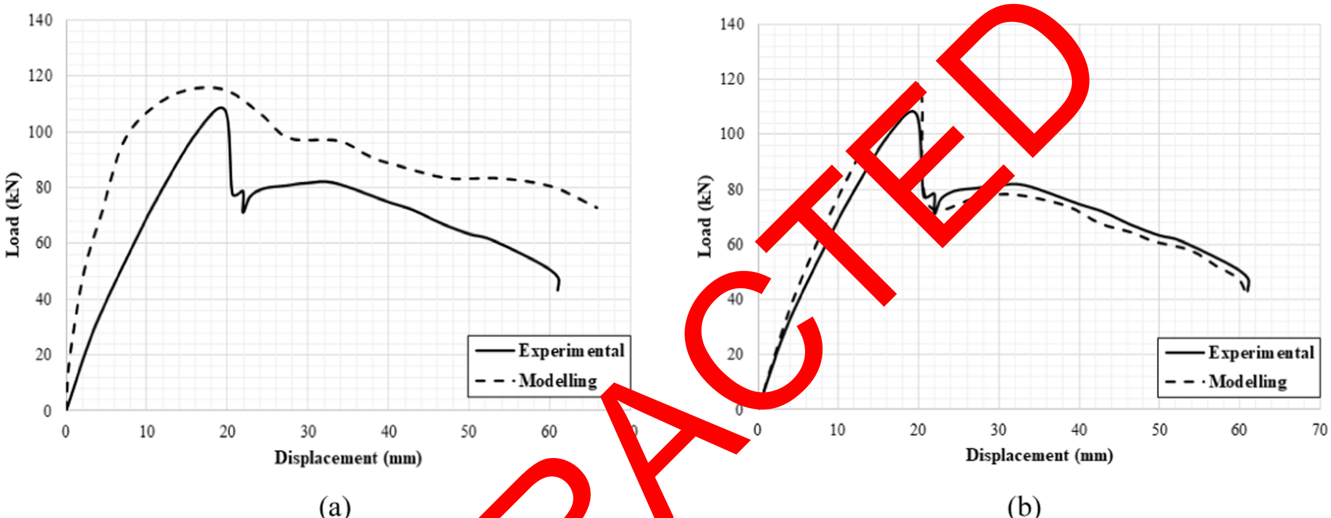

Fig. 22. Load-displacement relationship of the specimens with $0.8l_d$ and without SF a) with no-slip and b) with slip.

$$d_t = 1 - \frac{\sigma}{f_t} \tag{8}$$

where σ and f_t indicate the stress at each step and tensile strength of concrete, respectively.

Furthermore, the translator element was incorporated into the finite element model to simulate bond action and consider the slip-force response between concrete and the rebars. The assigned translator element at the concrete-rebar interface consisted of two nodes, as presented in Fig. 19. The slippage at various interface locations was defined using nodes' relative displacement in the direction of slippage [50]. The properties of the reinforcement were used according to the results of the

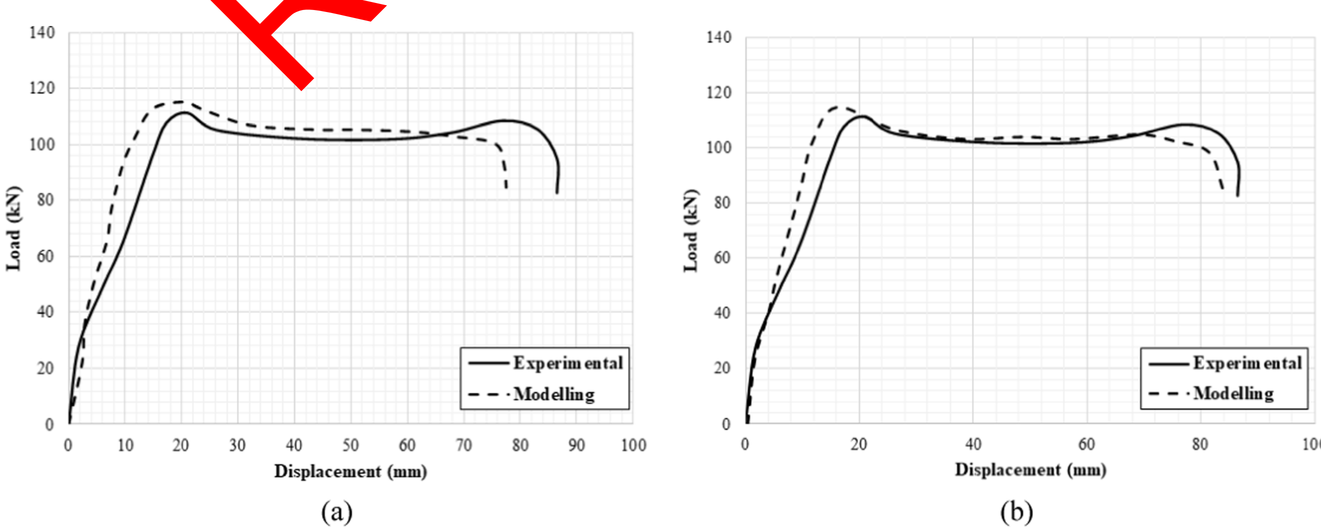

Fig. 23. Load-displacement relationship of the specimens with $0.8l_d$ and 2% SF a) with no-slip and b) with slip.

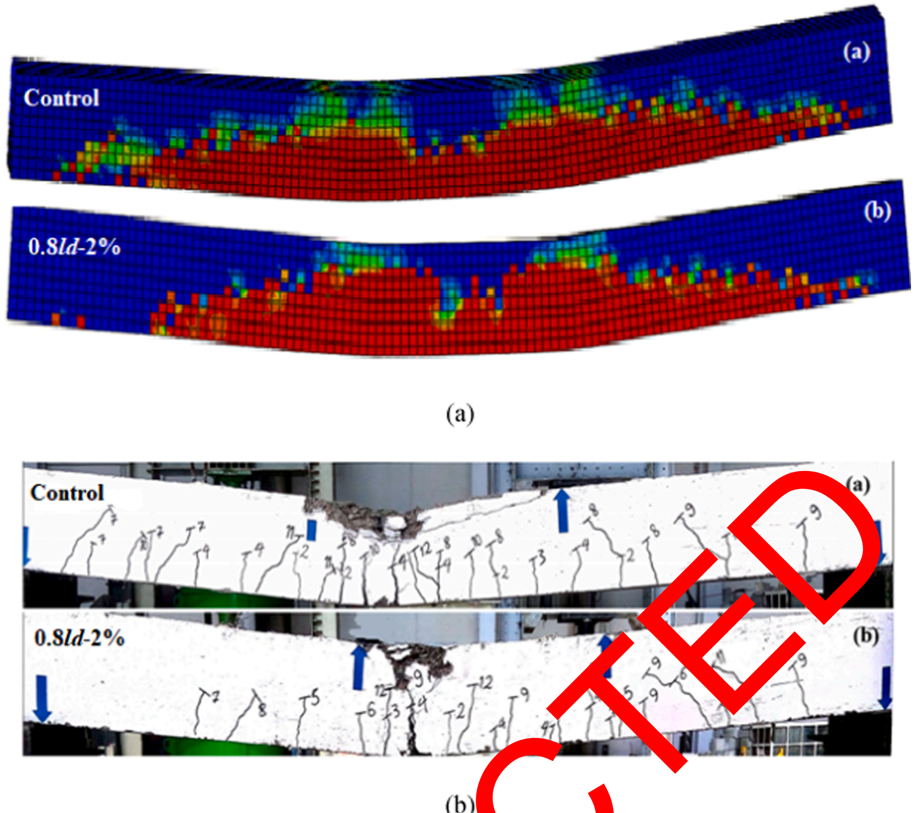

Fig. 24. Cracks propagation and failure mode of the specimens a) numerically and b) experimentally.

direct tensile test. The non-slip mode was also considered to simulated the interaction of concrete and reinforcement in the cases without slip. The translator elements were modelled as springs to allow the required degrees of freedom for slippage between the reinforcement and concrete subjected to the axial and lateral forces. According to the [illegible] code, the bond stress-slip relation for ribbed bars was defined according to Fig. 20 and Eq. (9) [51].

$$\tau_b = \begin{cases} \tau_{b.max}\left(\frac{S}{S_1}\right)^{\alpha} 0 \le S \le S_1 \\ \tau_{b.max} S_1 \le S \le S_2 \\ \tau_{b.max} - \frac{\tau_{b.max} - \tau_f}{S_2 - S_3}(S - S_3) S_2 \le S \le S_3 \\ \tau_f S_3 \le S \le S_4 \\ 0 S \ge S_4 \end{cases} \tag{9}$$

where τ_b, S, $\tau_{b.max}$, and τ_f are the bond stress, slip, maximum bond stress, and lower constant level (=40% of $\tau_{b.max}$), respectively. Moreover, S1 ~ S4 are the model parameters that were considered according to previous studies [52]. In this study, the effect of transverse reinforcement spacing along the lap-spliced region and longitudinal tensile rebars ratio on the flexural behaviour and ductility of RC beams with different lap-splice lengths and SF contents was analysed. In addition, the cross-section dimension of all specimens was kept constant. The specimen's specifications are presented in Table 5.

7.2. Verification

In this section, two plain and SFRC specimens considering with and without slip were calibrated using existing experimental data - to ascertain the validity of the used numerical model. As also mentioned above, to correctly define the behaviour of materials, the stress–strain relationship of materials was defined in the software. Fig. 21 shows the conducted simulation in ABAQUS software with slip (with connector) and without slip. Additionally, according to the low slip between the transverse reinforcement and concrete in RC beams, the slip for transverse reinforcement was neglected and a tie element (embedded state) was utilized for transverse reinforcement [42-45].

To perform the simulation, the analysed model was verified against the conducted experiments on the specimens. Figs. 22 and 23 compare the load–displacement responses of specimens with different lap-splice lengths, SF contents and slips - according to experimental and simulation results. There, ignoring the slip between the rebars and concrete (embedded region) led to considerable error between the experimental and analytical results by simulation when SF were not used because the slip value is large in plain concrete beams. Conversely, the embedded region with no-slip could be considered with acceptable performance when 2% SF were added because the bond resistance increased and the slip between the longitudinal tensile rebars and concrete significantly declined. However, considering the slip between the rebar and concrete gave high accurate results, relative to the experimental results. Therefore, the results showed the accuracy and efficiency of the simulation and the presented models could be utilized for both plain and SF concrete beams.

Additionally, cracking and its propagation was compared, as presented in Fig. 24, which also shows the accuracy of the simulation in terms of the flexural behaviour of SFRC beam with lap-spliced bars. After the verification, the influence of the longitudinal tensile rebars ratio and transverse reinforcement spacing along the splice length on the flexural performance of ductility of SFRC beams with different lap-splice lengths (l_d, 0.8l_d and 0.6l_d).

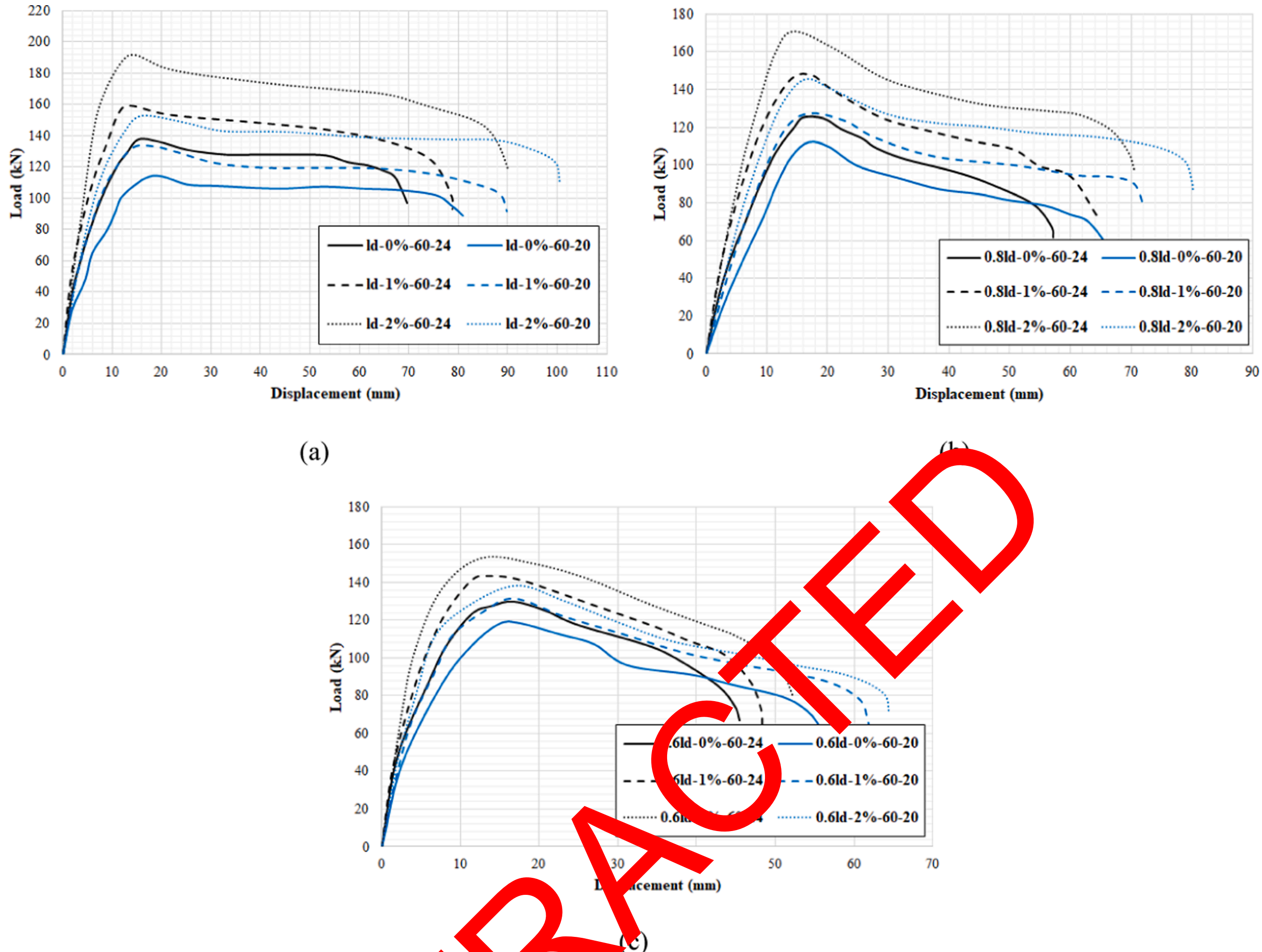

Fig. 25. Influence of longitudinal tensile rebar ratio on the load-displacement relationship of SFRC beams with lap-spliced bars a) l_d, b) $0.8l_d$ and c) $0.6l_d$.

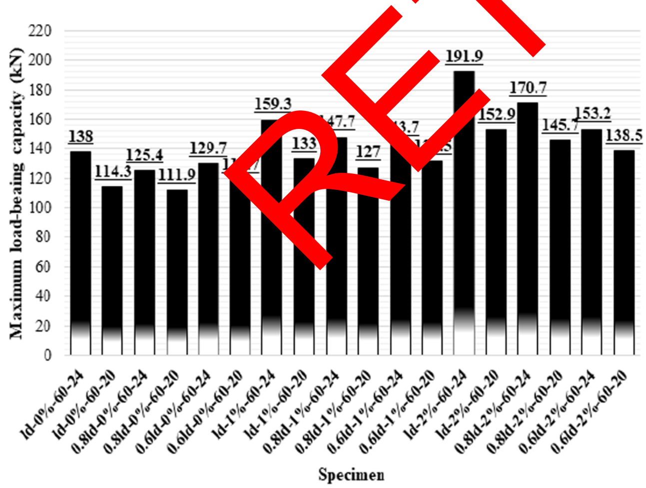

Fig. 26. Influence of longitudinal tensile rebar ratio on the maximum capacity of SFRC beams with lap-spliced bars.

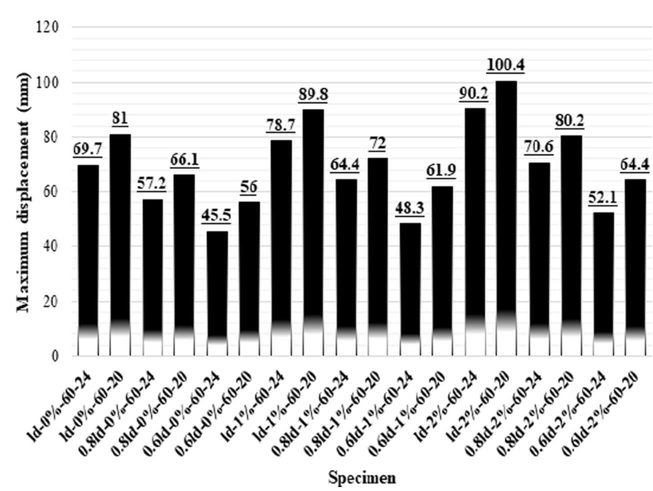

Fig. 27. Influence of longitudinal tensile rebar ratio on the maximum deformation of SFRC beams with lap-spliced bars.

7.3. Load-displacement and ductility of the specimens

7.3.1. Influence of longitudinal tensile rebar ratio

Fig. 25 shows the influence of longitudinal tensile rebar ratio on the load–displacement performance of RC beams with lap-spliced bars and different SF contents. There, the flexural strength increased and the maximum deformation declined with an increase in longitudinal tensile rebar ratio. Moreover, with the use of SF, both the maximum load-bearing capacity and mid-span displacement of RC beams with various lap-splice length improved. The effect of SF on improving the

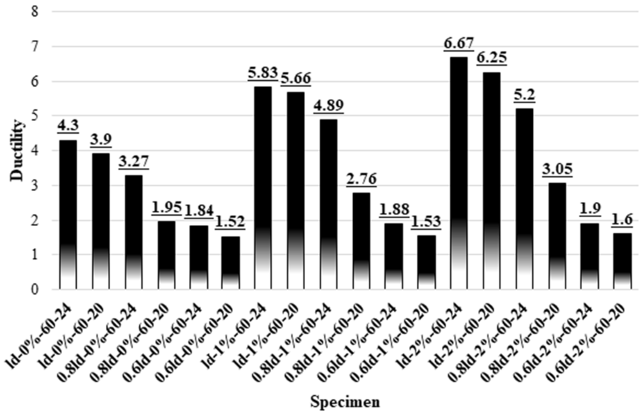

Fig. 28. Influence of longitudinal tensile rebar ratio on the ductility of SFRC beams with lap-spliced bars.

performance of RC beams with a higher longitudinal rebar ratio was greater. This could be attributed to a higher confinement area around the rebars with an increase in their diameter due to increasing the bond resistance between the longitudinal tensile rebars and concrete. Regarding Fig. 25, the addition of SF played an effective role in significantly improving the maximum bearing capacity of the RC beam when the required lap-splice length was cut by 20% ($0.8l_d$). The improvement influence of SF on the behaviour of specimens declined and, when the lap-splice length declined by 40%, the use of SF had an insignificant influence on maximum flexural strength and deformation of RC beams. Therefore, the lap-splice length could be cut by 20% when SF were added. It should be stated that adding SF does not have a significant influence on improving the performance of RC beams, and at least $0.8l_d$ lap-splice length should be provided when SF are added. Additionally, increasing the longitudinal rebar ratio did not considerably affect the load-bearing capacity of RC beams when the lap-splice length declined by a high percentage (40%) due to a substantial drop in bond resistance between the tensile rebar and concrete.

Furthermore, the maximum load-bearing capacity and mid-span displacement of the specimens are presented in Figs. 26 and 27, respectively. According to Fig. 21, the strength of RC beams with the required lap-splice length (l_d) improved by 39.3% and 67.8% when the longitudinal rebars ratio increased by 1% and respectively 1% and 2% SF were added. Conversely, the maximum deformation improved by 28.8% and 44.1% when the longitudinal rebars ratio decreased by 1% and respectively 1% and 2% SF were used.

The effect of longitudinal tensile rebar ratio on the ductility of SFRC beams with various lap-splice length is provided in Fig. 28. According to

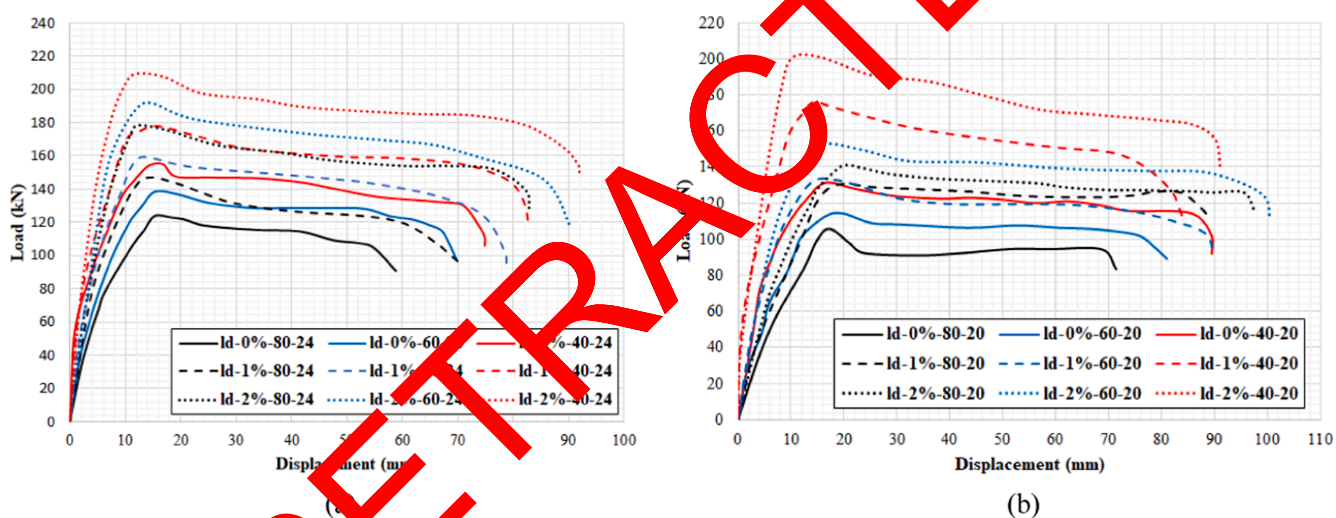

Fig. 29. Influence of transverse reinforcement spacing along the lap-splice length on the load–displacement relationship of SFRC beams with l_d lap-spliced bars.

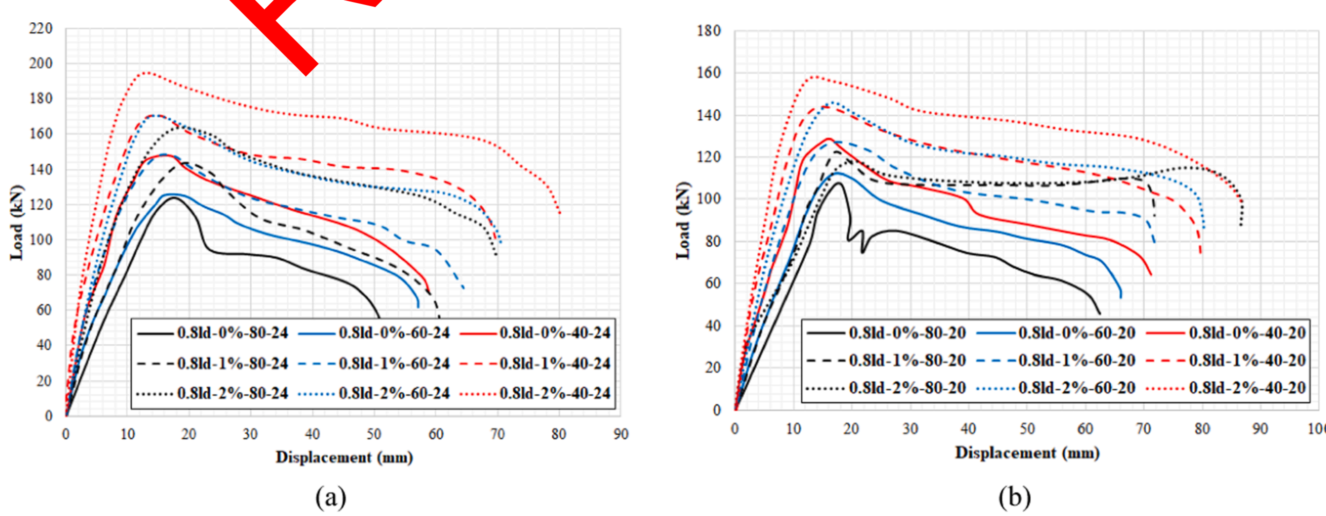

Fig. 30. Influence of transverse reinforcement spacing along the lap-splice length on the load–displacement relationship of SFRC beams with $0.8l_d$ lap-spliced bars.

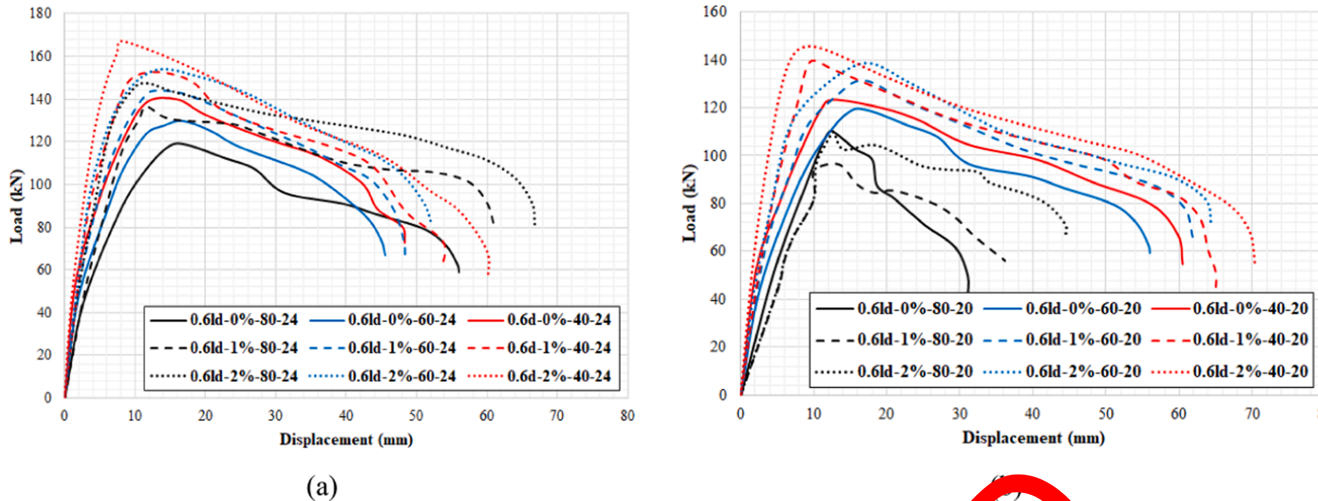

Fig. 31. Influence of transverse reinforcement spacing along the lap-splice length on the load–displacement relationship of SFRC beams with $0.6l_d$ lap-spliced bars.

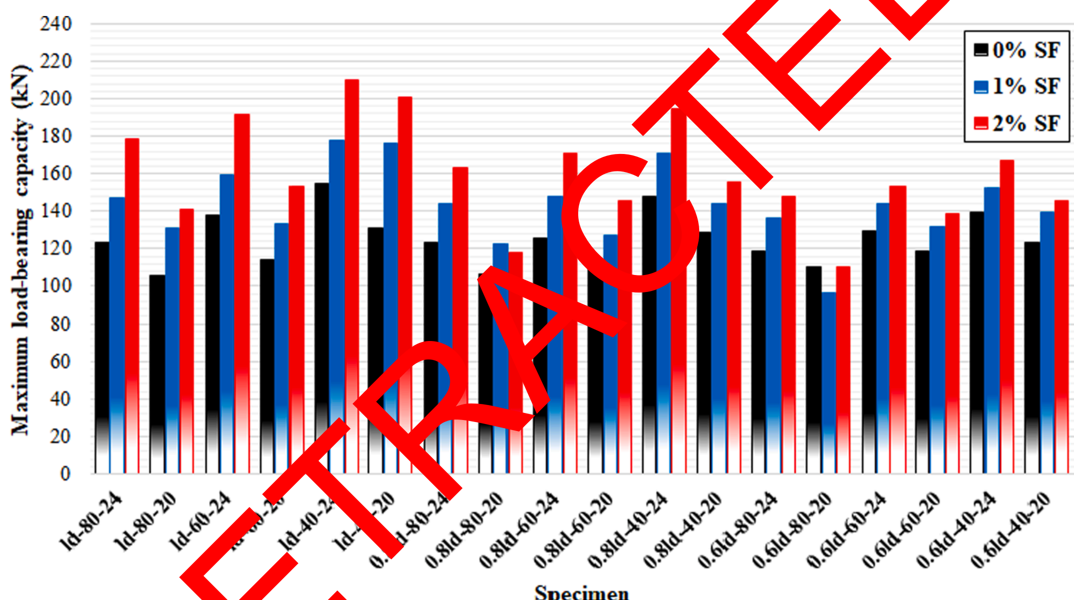

Fig. 32. Influence of transverse reinforcement spacing along the lap-splice length on the maximum capacity of SFRC beams with lap-spliced bars.

this figure, the ductility of RC beams declined with a reduction in lap-splice length. Moreover, the incorporation of SF improved the ductility due to raising the bond resistance between the tensile rebar and concrete, and transferring the stress along the cracks' width. Additionally, reducing the diameter of the longitudinal tensile rebars led to reducing the ductility of the specimens. In addition, using SF significantly improved the ductility of RC beams with lap-spliced bars when higher diameter rebar was used for longitudinal tensile rebars. The addition of SF did not significantly improve the ductility of the RC-beam with lap-splice length when both splice length and tensile rebars ratio decreased. Therefore, for those specimens with l_d lap-splice length, the increase in longitudinal tensile rebar diameter with 1% and 2% SF improved the ductility respectively by 49.4% and 60.2%. In addition, when a higher longitudinal tensile rebar ratio (with 24 mm diameter or 3% longitudinal ratio) with $0.8l_d$ was used, the addition of 1% and 2% SF improved the ductility respectively by 13.7% and 20.9% in comparison with the specimen with the required splice length (l_d) and without SF ($l_d - 0\% - 60 - 24$). In other cases, the ductility considerably declined with a reduction in lap-splice length, even if SF were added. Thus, the minimum reduction of 61%, 60% and 58% was observed when the lower longitudinal tensile rebar ratio with $0.6l_d$ lap-splice length was used with 0%, 1% and 2% SF, respectively.

7.3.2. Influence of transverse reinforcement spacing along the lap-splice length

In this section, the influence of transverse reinforcement along the splice length on the flexural responses and ductility of RC beams was numerically investigated. The results are presented in Figs. 29 and 30 for different lap-splice lengths and diameters of the longitudinal tensile rebar. There, the reduction in transverse reinforcement spacing along the splice length improved the load-bearing capacity and deformation of RC beams with various lap-splice lengths. Therefore, providing adequate transverse reinforcement is important to provide an appropriate load–displacement behaviour of RC beams with lap-spliced bars, while the improvement influence on the flexural strength increased with an increase in longitudinal rebar ratio. This could be attributed to increasing the confinement strength around the rebars and the bond resistance with an increase in longitudinal rebar ratio. Conversely, the improvement effect of reducing transverse reinforcement spacing declined with a reduction in lap-splice length. Therefore, a slight

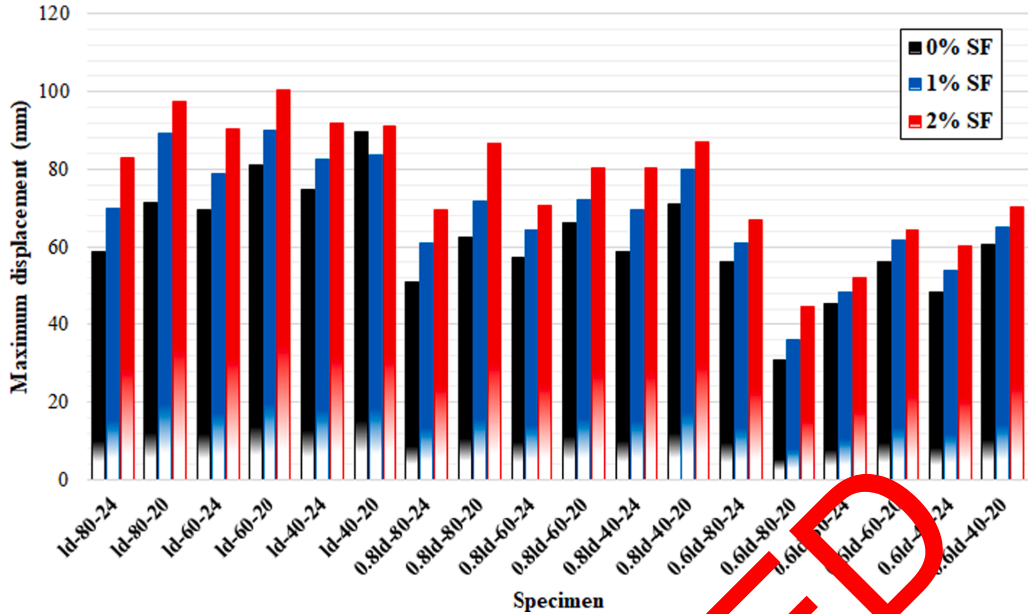

Fig. 33. Influence of transverse reinforcement spacing along the lap-splice length on the maximum deformation of SFRC beams with lap-spliced bars.

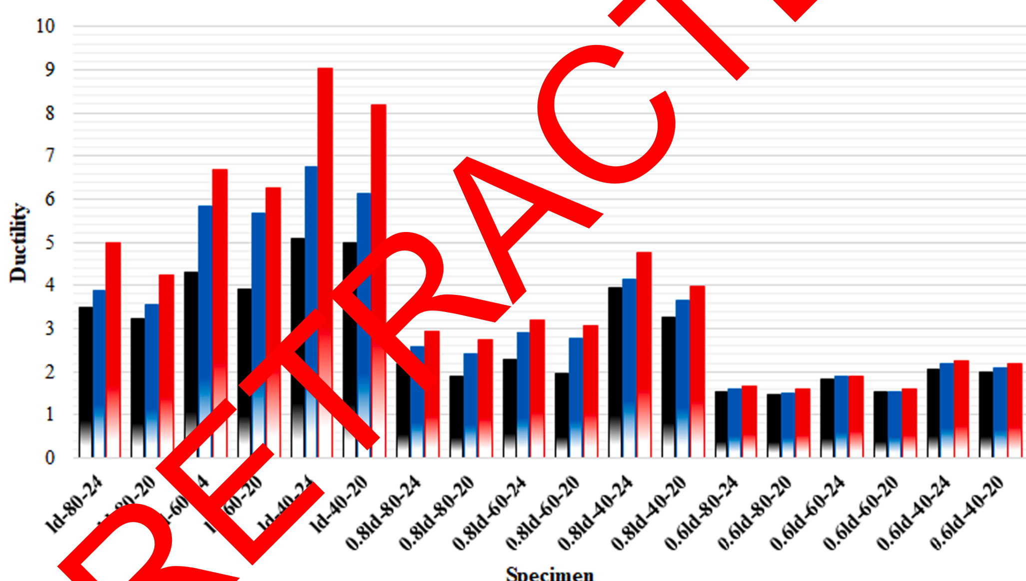

Fig. 34. Influence of transverse reinforcement spacing along the lap-splice length on the ductility of SFRC beams with lap-spliced bars.

enhancement in the load–displacement performance of RC beams as a result of a reducing transverse reinforcement spacing was observed when the lap-splice length declined by 40% ($0.6l_d$). According to Figs. 29 and 31, the lap-splice length could be cut by 40% when the transverse reinforcement spacing along the splice length was halved and 2% SF were added. Furthermore, the values of maximum load-bearing capacity and deformation are shown in Figs. 29 and 30, respectively.

According to Fig. 32, in specimens with 2% tensile rebar ratio, the maximum strength of RC beams improved by 29.1% and 16.7% when the lap-splice length declined respectively by 20% and 40%, and 2% SF were added, relative to the same specimen with the required lap-splice length ($l_d - 0\% - 80 - 20$). In addition, in the beams with 3% tensile rebar ratio, the splice length declined by 20% and 40% but the ultimate load-bearing capacity improved by 58.3% and 417% when 2% SF were added and the stirrup spacing along the splice length was halved. Additionally, in the beams with 2% and 3% tensile rebar ratio and $0.8l_d$ lap-splice length, the maximum mid-span displacement improved respectively by 33% and 22% when 2% SF were added (Fig. 33).

Fig. 34 provides the influence of transverse reinforcement spacing on the ductility of RC beams with various lap-splice lengths, SF contents and longitudinal tensile rebar ratios. There, the reduction in transverse reinforcement spacing along the splice length played an important role in improving the ductility of the RC beam when sufficient lap-splice length was provided (l_d), and the maximum improvement was obtained when 2% SF were also added. Therefore, the ductility improved by 94% and 157% when 2% SF were used in RC beams with 3% tensile rebars ratio and the transverse reinforcement spacing was cut by 20 mm and 40 mm, respectively. Additionally, in 2% SFRC beams with 2% tensile rebar ratio, the ductility improved by 48.7% 100% when the transverse reinforcement spacing decreased by 20 mm and 40 mm along the splice length, respectively. Conversely, a reduction in transverse reinforcement spacing did not significantly improve the ductility of the specimen when the lap-splice length decreased, especially if a high percentage reduction (40% in this study) was performed. However, the addition of SF significantly enhanced the ductility, particularly when 2% SF were added.

8. Conclusions

In this study, the effects of different parameters including SF content, lap-splice length, longitudinal tensile rebar ratio and transverse reinforcement spacing along spliced bars was experimentally and numerically investigated. Following the experimental results, finite element method software, ABAQUS, was utilized and a novel simulation was developed to model the bond-slip behaviour of steel rebars in SFRC beams. Analysing the effect of using various parameters on the flexural responses and ductility of RC beams with lap-spliced bars considering slip between concrete and the tensile rebars was the prime objective of this study. According to the main results of this study, the following conclusion could be drawn:

1. The simulated flexural responses of the RC beam with lap-spliced agree well with its experimental behaviour, considering similar parameters in both the experimental and analytical approaches. Incorporating translator elements at the concrete-reinforcement interface enhances the precision of the conducted simulation. Therefore, the finite element method is a useful tool to model the bond-slip performance of rebars in both plain and fibre-reinforced concrete members;
2. In SFRC beams with SF contents above 1%, the slip between the rebars and concrete can be neglected and the embedded element (with no-slip) can be used to simulate the structural performance of RC beams;
3. The addition of SF significantly improved the strength and displacement of specimens when sufficient lap-splice length (l_d) was provided and the performance of the beam was further improved with increasing SF content. The reduction in lap-splice length led to reducing the maximum strength and deformation of beams while adding SF improved the performance of beams with reduced lap-splice length. However, with the use of SF, the lap-splice length could be cut by 20% with no reduction in the maximum load-bearing capacity of RC beams. Additionally, adding SF did not affect the structural performance of specimens when the lap-splice length declined by 40%;
4. The cracks width declined and they propagated more when SF were added. In addition, by reducing the lap-splice length, specimens failed suddenly with low deformation. Therefore, cracks concentrated at the spliced region. In addition, reducing the lap-splice length increased the width of cracks and the cracks were substantially increased when the lap-splice length declined by 40%. SF did not significantly decrease the cracks width in specimens with $0.6l_d$ the lap-splice length, which shows the importance of providing sufficient lap-splice length;
5. The addition of SF substantially improved the ductility of the specimens, but adding fibres did not considerably improve the ductility of RC beams with $0.6l_d$, and the ductility of beams decreased when the lap-splice length decreased;
6. Flexural strength improved and deformation decreased by increasing the longitudinal tensile rebar ratio. The influence of SF on improving the performance of RC beams further increased by increasing the tensile rebar ratio. Additionally, increasing the longitudinal rebar ratio did not significantly improve the load-bearing capacity of RC beams when the lap-splice length declined by 40%;
7. Ductility declined by reducing the diameter of the tensile rebar ratio. Moreover, the addition of SF substantially improved the ductility of RC beams with lap-spliced bars when higher diameter longitudinal tensile rebars were used. However, the use of SF did not significantly improve the ductility of RC beam with lap-splice length when both the splice length and tensile rebars ratio decreased;
8. Reducing the transverse reinforcement spacing along the spliced bars improved the strength and deformation of RC beams with various lap-splice lengths. Therefore, providing sufficient transverse reinforcement is important to provide the proper behaviour of RC beams with lap-spliced bars. Moreover, the improvement influence on the flexural strength increased with an increase in longitudinal rebar ratio. Therefore, the lap-splice length could be cut by 40% when the transverse reinforcement spacing was halved and 2% SF were used, as well;
9. Reducing the transverse reinforcement spacing along the splice length played an important role in improving the ductility of the RC beam when sufficient lap-splice length was provided (l_d), while a reduction in transverse reinforcement spacing did not significantly improve the ductility of the specimen when the lap-splice length decreased by 40% ($0.6l_d$). However, the addition of SF significantly enhanced the ductility, especially when 2% SF were used.

CRediT authorship contribution statement

Arash Karimipour: Conceptualization, Methodology, Formal analysis, Data curation, Writing – original draft, Writing – review & editing. **Jorge de Brito:** Conceptualization, Methodology, Formal analysis, Data curation, Writing – review & editing. **Osman Gencel:** Conceptualization, Methodology, Formal analysis, Data curation, Writing – review & editing.

Declaration of Competing Interest

The authors declare that they have no known competing financial interests or personal relationships that could have appeared to influence the work reported in this paper.

Acknowledgements

The authors gratefully acknowledge the support of CERIS (Civil Engineering Research and Innovation for Sustainability) and FCT (Foundation for Science and Technology).

Data availability

The raw/processed data required to reproduce these findings cannot be shared at this time, as the data also is part of an ongoing study.

References

[1] Aydın E, Boru E, Aydın F. Effects of FRP bar type and fibre reinforced concrete on the flexural behaviour of hybrid beams. Constr Build Mater 2021;279:122407. https://doi.org/10.1016/j.conbuildmat.2021.122407.
[2] Özkılıç YO, Aksoylu C, Arslan MH. Experimental and numerical investigations of steel fibre reinforced concrete dapped-end purlins. J Build Eng 2021;36:102119. https://doi.org/10.1016/j.jobe.2020.102119.
[3] Rivera JE, Eid R, Paultre P. Influence of synthetic fibres on the seismic behaviour of reinforced-concrete circular columns. Eng Struct 2021;228:111493. https://doi.org/10.1016/j.engstruct.2020.111493.
[4] Liu J, Zhang J, Li X, Cao W. Cyclic behaviour of damage-controllable steel fibre-reinforced high-strength concrete reduced-scale frame structures. Eng Struct 2021;232:111810. https://doi.org/10.1016/j.engstruct.2020.111810.
[5] Meng G, Wu B, Xu S, Huang J. Modelling and experimental validation of flexural tensile properties of steel fibre reinforced concrete. Constr Build Mater 2021;273:121974. https://doi.org/10.1016/j.conbuildmat.2020.121974.
[6] Mahmood SMF, Foster SJ, Valipour H. Moment redistribution and post-peak behaviour of lightly reinforced-SFRC continuous slabs. Eng Struct 2021;232:111834. https://doi.org/10.1016/j.engstruct.2020.111834.
[7] Nematzadeh M, Fallah-Valukolaee S. Experimental and analytical investigation on the structural behaviour of two-layer fibre-reinforced concrete beams reinforced with steel and GFRP rebars. Constr Build Mater 2021;273:121933. https://doi.org/10.1016/j.conbuildmat.2020.121933.
[8] Karimipour A, Ghalehnovi M, de Brito J. Mechanical and durability properties of steel fibre-reinforced rubberised concrete. Constr Build Mater 2020;257:119463. https://doi.org/10.1016/j.conbuildmat.2020.119463.

[9] Fu C, Ye H, Wang K, Zhu K, He C. Evolution of mechanical properties of steel fibre-reinforced rubberized concrete (FR-RC). Compos B Eng 2019;160:158–66. https://doi.org/10.1016/j.compositesb.2018.10.045.

[10] Yuan TF, Lee JY, Min KH, Yoon YS. Experimental investigation on mechanical properties of hybrid steel and polyethene fibre-reinforced no-slump high-strength concrete. Int J Polym Sci 2019:256–74. https://doi.org/10.1155/2019/4737384.

[11] Olalusi OB, Awoyera PO. Shear capacity prediction of slender reinforced concrete structures with steel fibres using machine learning. Eng Struct 2021;227:111470. https://doi.org/10.1016/j.engstruct.2020.111470.

[12] Facconi L, Minelli F, Ceresa P, Plizzari G. Steel fibres for replacing minimum reinforcement in beams under torsion. Mater Struct/Materiaux et Constructions 2021;54:124–67. https://doi.org/10.1617/s11527-021-01615-y.

[13] Ghalehnovi G, Karimipour A, de Brito J, Chaboki HR. Crack width and propagation in recycled coarse aggregate concrete beams reinforced with steel fibres. Appl Sci 2020;10.

[14] Karimipour A, Ghalehnovi G. Comparison of the effect of the steel and polypropylene fibres on the flexural behaviour of recycled aggregate concrete beams. Structures 2021;29:129–46.

[15] Karimipour A, Mohebbi Najm Abad J, Fasihihour N. Predicting the load-carrying capacity of GFRP-reinforced concrete columns using ANN and evolutionary strategy. Compos Struct 2021;275:114470.

[16] Karimipour A, Ghalehnovi G, de Brito J. Effect of micro polypropylene fibres and nano TiO2 on the fresh- and hardened-state properties of geopolymer concrete. Constr Build Mater 2021;300:124239.

[17] Li B, Xu L, Shi Y, Chi Y, Liu Q, Li C. Effects of fibre type, volume fraction and aspect ratio on the flexural and acoustic emission behaviours of steel fibre reinforced concrete. Constr Build Mater 2018;181:474–86. https://doi.org/10.1016/j.conbuildmat.2018.06.065.

[18] Biolzi L, Cattaneo S. Response of steel fibre reinforced high strength concrete beams: experiments and code predictions. Cem Concr Compos 2017;77:1–13. https://doi.org/10.1016/j.cemconcomp.2016.12.002.

[19] Lee JY, Oh Shin H, Yeol Yoo D, Soo Yoon Y. Structural response of steel-fibre-reinforced concrete beams under various loading rates. Eng Struct 2018;156(1):271–83. https://doi.org/10.1016/j.engstruct.2017.11.052.

[20] Ranjbaran F, Rezayfar O, Mirzababai R. Experimental investigation of steel fibre-reinforced concrete beams under cyclic loading. Int J Adv Struct Eng 2018;10:49–60. https://doi.org/10.1007/s40091-018-0177-1.

[21] Roesler JR, Altoubat SA, Lange DA, Rieder KA, Ulreich GR. Effect of synthetic fibres on the structural behaviour of concrete slabs-on-ground. ACI Mater J 2006;103(1):3–10.

[22] Soutsos MN, Le TT, Lampropoulos AP. Flexural performance of fibre reinforc[illegible] concrete made of steel and synthetic fibres. Constr Build Mater 2012;36:704–[illegible]. https://doi.org/10.1016/j.conbuildmat.2012.06.042.

[23] Karimipour A, de Brito J. Influence of polypropylene fibres and silica fume on th[illegible] mechanical and fracture properties of ultra-high-performance geo[illegible] concrete. Constr Build Mater 2021;283:122753. https://doi.org[illegible]0.1016/[illegible]conbuildmat.2021.122753.

[24] Yalciner H, Kumbasaroglu A, El-Sayed AK, Pekrioglu Balk[illegible] A, [illegible] Turan A[illegible], et al. Flexural strength of corroded reinforced concrete [illegible]ams. Str[illegible] J 2020;117:29–41.

[25] Rezaiee-Pajand M, Karimipour A, Mohebbi Najm [illegible]d J. [illegible]ack spacing [illegible]diction of fibre-reinforced concrete beams with lap-spliced bars by [illegible]chine learning models. Iran J Sci Technol Trans Civil Eng. [illegible]20;15:35–46. h[illegible]://link.springer.com/article/10.1007/s40996-020-00441[illegible]

[26] Ghalehnovi M, Farokhpour Tabrizi M, [illegible]rimipou[illegible]. Investigation of the effect of steel fibres on failure extension of recyc[illegible] ag[illegible]egate con[illegible]rete beams with lap-spliced bars. Sharif J Civil Eng 20[illegible]18:12[illegible]ps://doi[illegible]g/10.24200/j30.2019.52894.2513.

[27] Karimipour A, Esfahani MR[illegible]he effect[illegible]f steel fib[illegible]on flexural cracking of fibre in reinforced concrete beam[illegible]ith lap[illegible]bars. Ferdowsi Univ J Civil Eng 2017;31:25–37. https://doi.org/1[illegible]/civil.v3[illegible].62182.

[28] Karimipour A, Edalati M, de Br[illegible]J. Biaxial mechanical behaviour of polypropylene fibres reinforced se[illegible]compacting concrete. Constr Build Mater 2021;278:122416. https://doi.org/1[illegible]1016/j.conbuildmat.2021.122416.

[29] Azizinamini A, Darwin D, Eligehausen R, Pavel R, Ghosh SK. Proposed modifications to ACI 318–95 tension development and lap splice for high-strength concrete. ACI Struct J 1999;96(6):922–7.

[30] ACI 318-14. Building code requirements for structural concrete and commentary. Farmington Hills, MI, USA: ACI Committee 318, American Concrete Institute; 2014.

[31] Karimipour A. Effect of untreated coal waste as fine and coarse aggregates replacement on the properties of steel and polypropylene fibres reinforced concrete. Mech Mater 2020;150:103592. https://doi.org/10.1016/j.mechmat.2020.103592.

[32] Ghalehnovi M, Karimipour A, de Brito J. Influence of steel fibres on the flexural performance of reinforced concrete beams with lap-spliced bars. Constr Build Mater 2019;229:116853. https://doi.org/10.1016/j.conbuildmat.2019.116853.

[33] Karimipour A, Rakhshanimehr M, Ghalehnovi M, de Brito J. Effect of different fibre types on the structural performance of recycled aggregate concrete beams with spliced bars. J Build Eng 2021;38:102090. https://doi.org/10.1016/j.jobe.2020.102090.

[34] Chaboki HR, Ghalehnovi M, Karimipour A, de Brito J. Experimental study on the flexural behaviour and ductility ratio of steel fibres coarse recycled aggregate concrete beams. Constr Build Mater 2018;186:400–22. https://doi.org/10.1016/j.conbuildmat.2018.07.132.

[35] Gaurav G, Singh B. Bond strength prediction of tension lap splice for deformed steel bars in recycled aggregate concrete. Mater Struct/Materiaux et Constructions 2017;50:142–56. https://doi.org/10.1617/s11527-017-1101-z.

[36] Hu B, Wu YF. Quantification of shear cracking in reinforced concrete beams. Eng Struct 2017;147:666–78. https://d[illegible]/10.1016/j.engstruct.2017.06.035.

[37] Yoo DY, Moon DY. Effect of ste[illegible]ibres o[illegible]e flexural behaviour of RC beams with very low reinforcement rati[illegible] Constr Buil[illegible]ater 2018;188:237–54. https://doi.org/10.1016/j.conbuildmat.2[illegible]18.08.099.

[38] Rezaiee-Pajand M, Ka[illegible]ipour [illegible] Attari M. [illegible]precise splice length model for reinforced concrete[illegible]ructures. Pr[illegible]Inst C[illegible] Eng - Struct Build 2020;50:87–98. https://doi.org/1[illegible]1680/jst[illegible].19.00[illegible]

[39] Esfahani MR, K[illegible]oush M[illegible]. Development/splice length of reinforcing bars. ACI Struct J 20[illegible];102:[illegible]. https://[illegible].org/10.14359/13527.

[40] Cohn M[illegible] Bartlett M. [illegible]mpute[illegible]mulated flexural tests of partially prestressed concr[illegible]tions. J Stru[illegible] D[illegible] 1982;108:2747–65. https://doi.org/10.1061/jsd[illegible]g.000[illegible]3.

[41] ASTM C496/C[illegible]6M. Standard test method for splitting tensile strength of c[illegible]ndrical concr[illegible] specimens. West Conshohocken, U.S.A: ASTM International; 2017.

[42] BS EN 12[illegible]90 1. Testing hardened concrete: shape, dimensions and other requireme[illegible]ts for specimens and moulds. British Standards Institution; 2000.

[[illegible]] BS EN 12[illegible]90-3. Testing hardened concrete: Compressive strength of test specimens [illegible] B[illegible]sh Standards Institution; 2009.

[44] BS EN 12390-2. Testing hardened concrete: Making and curing specimens for strength tests, British Standards Institution; 2000.

[45] ASTM C469 / C469M-14e1. Standard Test Method for Static Modulus of Elasticity and Poisson's Ratio of Concrete in Compression. West Conshohocken, PA: ASTM International; 2014.

[46] Ran J, Li T, Chen D, Shang L, Li W, Zhu Q. Mechanical properties of concrete reinforced with corrugated steel fiber under uniaxial compression and tension. Structures 2021;34:1890–902.

[47] Al-Osta MA, Isa MN, Baluch MH, Rahman MK. Flexural behaviour of reinforced concrete beams strengthened with ultra-high performance fibre reinforced concrete. Constr Build Mater 2017;134:279–96. https://doi.org/10.1016/j.istruc.2021.04.004.

[48] Kwan AKH, Chu SH. Direct tension behaviour of steel fibre reinforced concrete measured by a new test method. Eng Struct 2018;176:324–36.

[49] Kaw Kk. Mechanics of composite material, 2nd ed. Tayler & Francis Group, The Academic Division of T&F Information Plc; 2006.

[50] Issa CA, Masri O. Numerical simulation of the bond behavior between concrete and steel reinforcing bars in specialty concrete. Int J Civil, Environ, Struct Constr Archit Eng 2015;9:6. https://doi.org/10.5281/zenodo.1109663.

[51] fib. Model Code. Switzerland: International Federation for Structural Concrete; 2010.

[52] Teng JG. Behavior and strength if FRP strengthened RC structures: a state of the art review. Proc Inst Civil Eng - Struct Build 2003;156(1):51–62. https://doi.org/10.1680/stbu.2003.156.1.51.